Investigating dynamic functional connectivity in a rat model of temporal lobe epilepsy

Yi Li

Supervisors: Prof. Christian Vanhove, Dr. Benedicte Descamps
Counsellor: Emma Christiaen

Master's dissertation submitted in order to obtain the academic degree of
Master of Science in Biomedical Engineering

Department of Electronics and Information Systems
Chair: Prof. dr. ir. Koen De Bosschere
Faculty of Engineering and Architecture
Academic year 2017-2018

GHENT
UNIVERSITY

Preface

This master thesis was written to complete the Master of Science in Biomedical Engineering. I want to thank all the people who have helped me this year.

First of all, I want to thank Emma Christiaen. Thank you for helping me to perform the experiment part and helping me with the data analysis, and for your patient guidance and advice.

I would like to thank professor Christian Vanhove and Benedicte Descamps for the help with the functional MRI imaging.

Finally, I would like to thank my parents for their support and help to make me insist on my study and never give up.

Yi Li
August 2018, Ghent

Investigating dynamic functional connectivity in a rat model of temporal lobe epilepsy

Yi Li

Supervisor(s): Emma Christiaen, Benedicte Descamps, Christian Vanhove

Abstract

Epilepsy is a group of neurological disorders and resting state fMRI has been used to investigate epilepsy. Functional connectivity can be used for the functional dependence between two regions of interest, and it is time-varying instead of stationary in reality, so dynamic functional connectivity is proposed. The aim of this study is to investigate the patterns of functional connectivity in epileptic rats and compare them with healthy rats. In this study, we used the intraperitoneal kainic acid rat model (Hellier protocol [1]) for temporal lobe epilepsy, and six epileptic rats and six healthy rats are used in this study. We can obtain resting state fMRI data six weeks after status epilepticus with 7T scanner using medetomidine anesthesia. Several preprocessing steps have been completed at first. Sliding window technique is the method we have applied to obtain dynamic functional connectivity (dFC). We can find the correlation coefficient varies over time, and k-means clustering characterizes seven states of functional connectivity. From the results of statistical analysis, we can find that the state of the lowest functional connectivity occurs more in epileptic rats, and the number of transitions of the states in healthy rats is higher than epileptic rats. In conclusion, the brains of epileptic animals are more often in the state of lower functional connectivity than the brains of healthy animals, and healthy animals have higher number of transitions of the states than epileptic ones. Further research is recommended to investigate dFC with more complex and informed model rather than correlation. This can provide more insight in the pathophysiology of epilepsy.

Keywords: Epilepsy, dynamic functional connectivity (dFC), resting state fMRI, intraperitoneal kainic acid rat model, sliding technique, k-means clustering

Investigating dynamic functional connectivity in a rat model of temporal lobe epilepsy

Yi Li
Supervisor(s): Emma Christiaen, Benedicte Descamps, Christian Vanhove

Abstract—**Epilepsy is a group of neurological disorders and resting state fMRI has been used to investigate epilepsy. Functional connectivity can be used for the functional dependence between two regions of interest, and it is time-varying instead of stationary in reality, so dynamic functional connectivity is proposed. The aim of this study is to investigate the patterns of functional connectivity in epileptic rats and compare them with healthy rats. In this study, we used the intraperitoneal kainic acid rat model (Hellier protocol [1]) for temporal lobe epilepsy, and six epileptic rats and six healthy rats are used in this study. We can obtain resting state fMRI data six weeks after status epilepticus with 7T scanner using medetomidine anesthesia. Several preprocessing steps have been completed at first. Sliding window technique is the method we have applied to obtain dynamic functional connectivity (dFC). We can find the correlation coefficient varies over time, and k-means clustering characterizes seven states of functional connectivity. From the results of statistical analysis, we can find that the state of the lowest functional connectivity occurs more in epileptic rats, and the number of transitions of the states in healthy rats is higher than epileptic rats. In conclusion, the brains of epileptic animals are more often in the state of lower functional connectivity than the brains of healthy animals, and healthy animals have higher number of transitions of the states than epileptic ones. Further research is recommended to investigate dFC with more complex and informed model rather than correlation. This can provide more insight in the pathophysiology of epilepsy.**

Keywords—**Epilepsy, dynamic functional connectivity (dFC), resting state fMRI, intraperitoneal kainic acid rat model, sliding technique, k-means clustering**

I. INTRODUCTION

Epilepsy is a group of neurological disorders and it has become a common disease all over the world. Epilepsy can be investigated using resting state fMRI. Resting state functional magnetic resonance imaging (RS-fMRI) has become a popular and important tool for investigating functional brain network.

In this study, an approach is described and implemented to assess the whole brain FC based on sliding window technique and k-means clustering of different correlation matrices. This method is applied to resting-state data from six epileptic rats and six healthy rats. We use k-means clustering to divide the matrices into different states and investigate patterns of FC that reoccur in time and across all the subjects. Statistical analysis is applied on the results to find the difference between epileptic and healthy rats and obtain the conclusion.

II. MATERIALS AND METHODS

A. Kainic acid (KA) rat model

In this experiment 12 adult male Sprague-Dawley rats (0.276 ± 0.019 body weight; Envigo, the Netherlands) are used. In this part, intraperitoneal kainic acid (IPKA) rat model was used to obtain epilepsy rats. KA injection according to the Hellier protocol, resulted in chronic epilepsy in all rats.

Kainate (5mg/kg) was administered to six healthy male Sprague-Dawley rats

intraperitoneally every hour until the animals displayed a stable status epilepticus (SE) for three hours, and control rats were treated similarity with saline. Seizures were determined by observing the behavioral postures. When we obtain the chronic epilepsy rats, for the next step.

B. Image acquisition

B.1 Anesthesia

The rat was anesthetized with 5% isoflurane mixed with 1.5L/min oxygen. And after this period, isoflurane was reduced to 2% mixed with 0.3L/min oxygen for maintenance during preparation for imaging. Then the neck of the rat was shaved and the needle (30G) was inserted under the skin for subcutaneous infusion of medetomidine. And next, the rat was placed on a heated water pad while in the magnet to maintain the temperature. A pressure sensor placed under the chest was used to continuously monitor breathing. After this step, the rat was given a bolus of medetomidine (0.05mg/kg) and after 10 minutes isoflurane was discontinued. Anesthesia was maintained with a constant medetomidine infusion rate (0.1mg/kg/h). After the image acquisition step, the anesthesia can be reversed with atipamezole.

B.2 Functional MRI acquisition

The resting-state fMRI images were acquired with a Pharmascan 7T (Bruker). Firstly, a wobble was done to match and tune radiofrequency coil. Then a tripilot scan was performed to get the information about the position of animal in the scanner. The magnetic field homogeneity can be improved by shimming. One TurboRARE T2 image of each rat was acquired after shimming. After that, the functional MRI images were acquired. About 30 minutes after turning off isoflurane, the resting-state fMRI images acquisition is performed using a standard gradient-echo echo planar imaging (EPI), with TR=2s, FOV=0.375mm, slice thickness/gap=1mm/0.1mm, scan matrix=80×80. This EPI imaging run is repeated 300 times in ten minutes and we can obtain 3 rsfMRI images.

C. Data analysis

Different analysis techniques and software are used to analyze fMRI images: statistical parametric mapping package (SPM12), sliding window technique with the toolbox GRETNA and k-means clustering performed by a script written in Matlab.

C.1 Preprocessing steps

The fMRI images are preprocessed using SPM12. Firstly, slice timing correction can be performed to adjust and correct for the time difference between different slices of the brain. Then, the different images have to be realigned to correct the data for the effects of movement during the scanning period. And next, the structural image is superimposed on a functional image to localize and visualize the active brain areas better in the coregistration step. After this step, the normalization step needs to be completed to normalize functional image to EPI template. In addition, the functional images are spatially smoothed with Gaussian filter with a size (FWHM) of 0.8mm to increase signal to noise ratio. In the last step, the bandpass filter at 0.01-0.1Hz is used to remove all non-neurological signals.

C.2 Static correlation analysis

One of techniques used to analyze the fMRI images is static correlation analysis, and the correlation coefficients are used in this kind of analysis. In the static correlation matrix, each row and each column represent a region of interest (ROI), and the elements are the correlation coefficients between each pair of ROIs to indicate the functional connectivity between these ROIs.

C.3 Sliding window technique

Sliding window technique can be used to obtain correlation matrices which vary over time. In this method, a time window of fixed length is selected, and the data points within this window are used to calculate correlation matrix of different regions of interest (ROIs). The window is shifted in time by a fixed step length which defines the overlap between two windows. Except for these fMRI images, a label mask of the rat brain is also necessary to achieve sliding window approach.

C.3.a Label mask of rat brain

After the preprocessing steps, we can obtain

three time series of preprocessed fMRI images for one subject. This label mask was made slice by slice by comparing with anatomical atlas to distinguish the different ROIs. And there are 38 ROIs in the rat brain fMRI image.

C.3.b Sliding window analysis

The optimal window length and step length were 50 seconds and 1TR(2s) which were used in this master thesis to obtain the final results. The whole process from label mask and fMRI data and sliding window approach was shown in Fig.1. When the optimal window length and step length are selected, each two of the signals within the window are used to calculate correlation coefficient, and all the correlation coefficients of different pairs of windowed signals can form one correlation matrix. After the window is shifted in time by a fixed window length, new correlation matrices can be obtained according to the same rule. Lastly, all the matrices are aggregated across subjects.

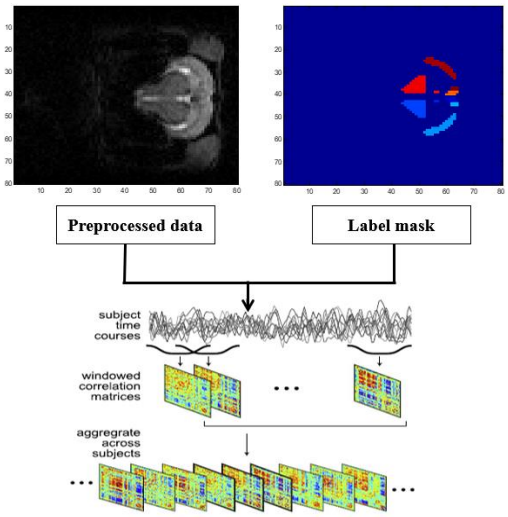

Fig.1. The overview of the analysis steps from the preprocessed data and the label mask

C.4 K-means clustering

K-means clustering algorithm was used to divide these dynamic FC matrices into separate clusters to observe the recurrence of patterns of dFC connectivity within subjects across time. An optimal k of 7 was obtained using elbow criterion method with the function in Matlab. There are 38 ROIs, so between each pair of ROIs, and we can obtain the FC matrix (38 × 38). The number of windows for each time course can be calculated as

$$\mathrm{WN} = \frac{(300-WL)}{SL} + 1 = 276.$$

There are six healthy and six epileptic (KA) rats in this experiment, and each subject has three sessions, so $276 \times 12 \times 3 = 9936$ instances need to be divided. These instances can be clustered to 7 states, so each functional connectivity matrix represents the centroid of a cluster and belongs to one state.

III. RESULTS

A. Static functional connectivity analysis

We can acquire the averaged correlation matrix for all healthy and epileptic rats separately, and the averaged correlation matrix over time for all epileptic rats and healthy rats is shown in Fig.2. From the comparison between these results, we can find visually the general values of correlation coefficients between many pairs of ROIs for healthy rats are higher than epileptic rats.

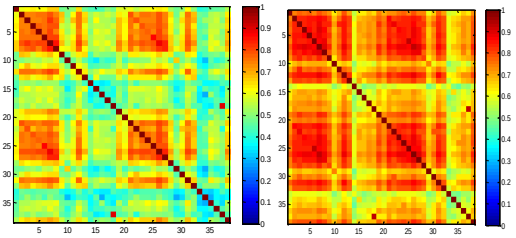

Fig.2. Averaged correlation matrix over time for all epileptic (left) and healthy (right) rats

B. Dynamic functional connectivity analysis

From the recent research, we can find that the functional connectivity between pairs of ROIs in rat brains are dynamic, so the correlation coefficient between two ROIs changes over time (window number), which is shown in Fig.3 This graph clearly shows that the correlation coefficient is not unchanged or static and it is varying over time, which can indicate the fact of dynamic functional connectivity.

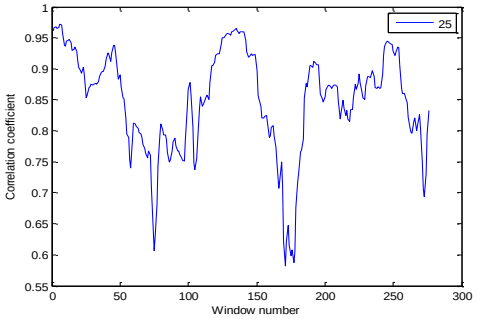

Fig.3. Correlation coefficient between two ROIs varies over window number

C. Sliding window technique

Sliding window technique is applied to obtain a series of correlation matrices. Sliding window technique was performed with GRETNA in this study.

D. Clustering

K-means clustering is used to cluster all the dynamic FC matrices for all scans including epileptic and healthy rats. The results of k-means clustering show that there are seven states for all dFC matrices, and the cluster centroids for FC states 1-7 are shown in Fig.4.

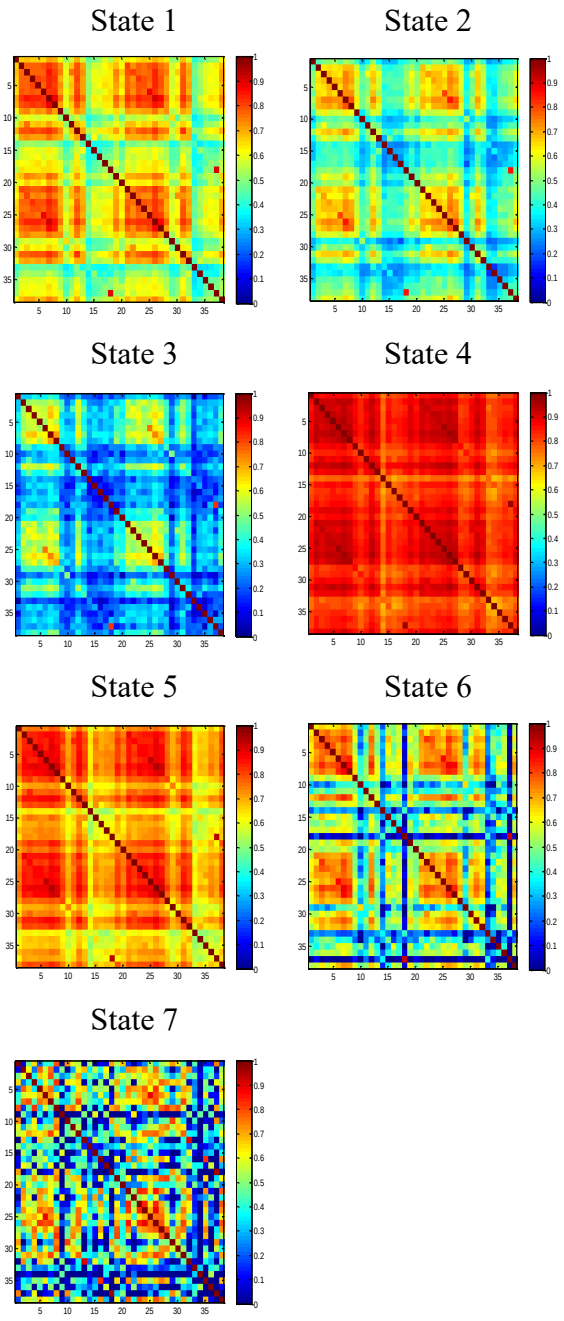

Fig.4. Correlation matrices of cluster centroids for FC States 1-7

We can clearly observe that there are huge differences of the values of correlation coefficients in these correlation matrices of seven states. We can find that stronger functional connectivity of all ROIs in State 1, State 4, State 5 and weaker functional connectivity of the ROIs in State 2, State 3, State 6 and State 7. From these connections, the two strongest correlations occur between left and right somatosensory cortex (SSC_l and SSC_r), and left septum and right septum (Sep_l and Sep_r) while left dorsolateral orbital cortex and temporal association cortex (DLO_l and TeA_l) exhibit a weaker correlation.

D.1 Total number and percentage of occurrences different states

When k-means clustering is completed to obtain seven states, the statistical calculation of the clustering results can be done. From the description above, we can know that 9936 instances in total need to be divided into seven states. We can obtain one graph to compare the number of occurrences different states clearly is shown in Fig.5.

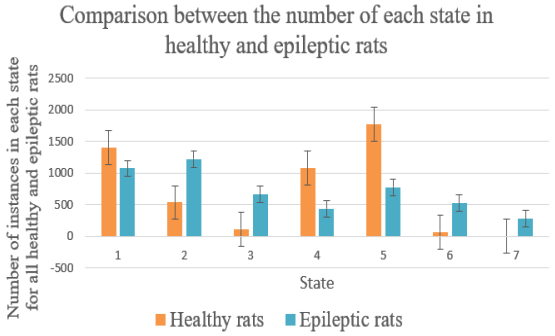

Fig.5. Comparison between the number of occurrences of each state in healthy and epileptic rats

From the graph above, we can find that the number and percentage of occurrences of healthy rats in State 1, State 4 and State 5 are much higher than epileptic rats and the number and percentage of occurrences of epileptic rats in State 2, State 3, State 6 and State 7 are much higher than healthy rats.

To complete the Mann-Whitney U test, p value is calculated for each state of the number of of epileptic and healthy rats, and all the p values of different states are shown in Table 1. There is a significant difference ($p<0.05$) of the number of

occurrences of State 3 between the epileptic and healthy rats. However, if the p<0.1, there is a trend towards significance or it is marginally significant, and it can indicate there is a marginally significant difference of the number of occurrences of that state between healthy and epileptic rats, such as the state 4 and state 5.

State	1	2	3	4	5	6	7
P	0.24	0.18	0.041	0.091	0.072	0.67	1

Table 1: P value of different states

There is a significant difference of the number of occurrences of State 3 between epileptic and healthy rats, and the number and percentage of occurrences of State 3 for epileptic rats are much higher than healthy rats. The mean value of correlation matrix in State 3 is much lower than other states, which indicates the weaker functional connectivity in State 3 than others.

D.2 Number of transients of states for each rat

Except for the number of different states, another important result which we can obtain from the k-means clustering is the number of transients of states for each rat. The transients of states indicate how frequency of the change of state. From the values of mean and standard deviation, we can find that the average number of transients in healthy rats is higher than epileptic rats.

For the statistical analysis, the Mann-Whitney U test can also be applied on the sum number of transitions of states for each rat. The p value which is calculated with this statistical test is 0.0649 ($0.05 < p < 0.1$), so we can't reject the null hypothesis without increasing the significance level, we can also find there is a marginally significant difference of the number of transitions of states between six healthy and epileptic rats.

IV. DISCUSSION

A. Functional connectivity in temporal lobe epileptic rats

In our study, for sFC analysis results, we can find the difference of mean value of correlation coefficients between these ROIs for healthy rats are higher than epileptic rats. For dFC analysis results, the matrix of State 3 has the lowest mean value of correlation coefficients compared to other states. The matrices of State 4 and 5 have the highest mean value of correlation coefficients compared to others. In addition, we have found left and right somatosensory cortex show stronger correlation than others, which is similar to this seen in previous work [2].

The current study compares the mean correlation matrix across all the subjects between healthy humans and epilepsy patients. And it reveals that the functional connectivity in the epilepsy patient group appeared to be less [3]. Other previous studies have found that cognitive and behavioral deficits are exhibited in epilepsy patients, such as attention, memory, and language function [4].

From the further investigation of the number and percentage of occurrences of different states, we have found the number and percentage of occurrences of State 3 of epileptic rats are much higher than healthy rats. Therefore, we can further infer that more dFC matrices of epileptic rats are divided into State 3 than healthy rats, and majority of epileptic rat brains have the same characteristic as the FC of State 3. This can indicate epileptic rat brains have weaker functional connectivity than healthy rats. In addition, the number and percentage of occurrences of State 4 and State 5 of healthy rats are higher than epileptic rats, so these two states with the highest correlation coefficients occur marginally significantly more in healthy rats than in epileptic rats.

For the transitions of functional connectivity, From the results, we have found the average number of transitions in healthy rats is higher than epileptic rats, which could indicate the healthy rat brains are more active than epileptic rats generally. The coefficient of variation and standard deviation of all healthy rats are lower than epileptic rats, which means the number of transitions of healthy rats is more stable and not changeable than epileptic rats.

One study found there was a significant difference in the number of transitions between seizure and healthy control, and total number of state transitions in patient was less than that of controls [5].

B. Optimal window length and step length

The choice of window size is an issue concerning the sliding window analysis. The window length should be short enough to permit the detection of fluctuations and long enough to allow estimation of FC [5]. In this study, the optimal window length of 50s and step length of 2s are chosen empirically based on the graph which obtained from the results and previous research [6]. There are some alternatives to a fixed window size, one may estimate the change points in FC to demarcate the windows, or use multi-scale window lengths approaches.

C. Limitations and future directions

Dynamic analysis is very sensitive to the noise, and the variations of the noise signal level across the scan which generate strong correlated signal fluctuations, can be wrongly seen as dynamic of functional connectivity. Another limitation is the white noise, which can exhibit the fluctuations in common FC matrices which are observed in actual fMRI data. Therefore, the sliding window technique should be accompanied by hypothesis which are supported with appropriate statistical testing.

Future work should consider multi-modal approaches such as EEG-fMRI, to determine the electrophysiological difference between FC states, and also to find the mapping of cognitive states from connectivity data.

V. CONCLUSION

In this study, the dynamic functional connectivity (dFC) is investigated using resting state fMRI (rs-fMRI) in a rat model of temporal lobe epilepsy. For static functional connectivity analysis, we can find visually the general values of correlation coefficients between ROIs for healthy rats are much higher than epileptic rats.

For the dynamic functional connectivity, we can obtain that the average values of correlation coefficients in State 1, State 4 and State 5 are higher than other states. Left and right somatosensory cortex shows the strongest correlation and dorsolateral orbital cortex and temporal cortex exhibits the weakest correlation in these high values states. Based on the statistical analysis, we have found the number and percentage of occurrences of State 3 for epileptic rats are much higher than healthy rats. Because the mean value of correlation matrix of State 3 is much lower than other states, we can infer that epileptic rat brains have weaker functional connectivity of these ROIs than healthy rat brains. For the number of transitions of states in healthy and epileptic rats, we can find the mean number of transitions in healthy rats is higher than epileptic rats.

The dynamic functional connectivity patterns of TLE rat models have been investigated and found in this study. Future research is recommended to investigate dFC with more complex and informed model rather than correlation using new multi-modal approaches and some techniques from other field.

REFERENCES

[1] Hellier J L, Patrylo P R, Buckmaster P S, et al., "Recurrent spontaneous motor seizures after repeated low-dose systemic treatment with kainate: assessment of a rat model of temporal lobe epilepsy," *Epilepsy Research 31,* pp. 73-84, 1998.

[2] Williams K A, Magnuson M, Majeed W, et al., "Comparison of α-chloralose, medetomidine and isoflurane anesthesia for functional connectivity mapping in the rat," Magnetic resonance imaging, pp. 995-1003, 2010.

[3] Luo C, Li Q, Lai Y, et al., "Altered functional connectivity in default mode network in absence epilepsy: a resting-state fMRI study," Human brain mapping, pp. 438-449, 2011.

[4] Henkin Y, Sadeh M, Kivity S, et al., "Cognitive function in idiopathic generalized epilepsy of childhood," Developmental medicine and child neurology, pp. 126-132, 2005.

[5] Liu F, Wang Y, Li M, et al., "Dynamic functional network connectivity in idiopathic generalized epilepsy with generalized tonic–clonic seizure," Human brain mapping, pp. 957-973, 2017.

[6] Shirer W R, Ryali S, Rykhlevskaia E, et al. , "Decoding subject-driven cognitive states with whole-brain connectivity patterns," Cerebral cortex, pp. 158-165, 2012.

Contents

List of abbreviations

AEDs	Anti-epileptic drugs
ATP	Adenosine triphosphate
BOLD	Blood oxygenation level dependent
CBF	Cerebral blood flow
CSF	Cerebral spinal fluid
CV	Coefficient of variation
dFC	Dynamic functional connectivity
EEG	Electroencephalography
EPI	Echo planer imaging
FC	Functional connectivity
fMRI	Functional magnetic resonance imaging
FWHM	Full width at half maximum
HRF	Hemodynamic response function
ICA	Independent component analysis
IP	Intraperitoneally
GE	Gradient echo
Gpe	Phase encoding gradient
Gro	Read out gradient
Gss	Slice select gradient
KA	Kainic acid
MRI	Magnetic resonance imaging
PD	Parkinson's disease
RF	Radio frequency
ROI	Region of interest
SD	Standard deviation
SE	Spin echo
sFC	Static functional connectivity
SPM	Statistical parametric mapping
TA	Acquisition time
TR	Repetition time
TE	Echo time
TLE	Temporal lobe epilepsy
TR	Repetition time

Chapter 1 Introduction

Epilepsy is a group of neurological disorders and it has become a common disease all over the world. Epilepsy can be investigated using resting state fMRI. Resting state functional magnetic resonance imaging (RS-fMRI) has become a popular and important tool for investigating functional brain network. Until recently, functional connectivity (FC) is usually assumed to stationary over the entire scan. However, if we focus on much smaller time scales, we can explore the dynamic properties of the fluctuations of spontaneous blood oxygenation level dependent signal.

In this study, an approach is described and implemented to assess the whole brain FC based on sliding window technique and k-means clustering of different correlation matrices. This method is applied to resting-state data from six epileptic rats and six healthy rats. The animal model for epilepsy which is used is the intraperitoneal kainic acid rat model for temporal lobe epilepsy. After the animal preparation steps, we can obtain resting-state fMRI data of these rats. All the preprocessing steps are performed using code written in Matlab (SPM and Gretna). The relationship and FC between different regions of interest are calculated and obtained with sliding window technique. A series of window length and step length are used to compare and find the optimal ones. Lastly, we use k-means clustering to divide the matrices into different states and investigate patterns of FC that reoccur in time and across all the subjects. Statistical analysis is applied on the results to find the difference between epileptic and healthy rats and obtain the conclusion.

Chapter 2 Literature study

2.1 Temporal lobe epilepsy

2.1.1 Introduction of epilepsy

Epilepsy is a group of neurological disorders characterized by recurrent spontaneous seizures [2]. A seizure is the clinical manifestation of an abnormal electrical activity of neurons within the brain [3]. The recurrence is very important for epilepsy, so a patient can only be diagnosed with epilepsy if he has had at least two unprovoked seizures [2].

2.1.2 Mechanism of epilepsy

The basic mechanism of neuronal excitability is the action potential. For a hyper-excitable state, it is caused by increased excitatory neurotransmission, reduced inhibitory neurotransmission, a change in voltage-gated ion channels instead of membrane depolarization [3]. An action potential occurs because of depolarization of the neuronal membrane, and with the depolarization propagating down in the axon to induce neurotransmitter release at the terminal of the axon. The neurotransmitters are the substances which are released by the axon terminal and bind to specific postsynaptic receptors [4].

Amino acid glutamate is the major excitatory neurotransmitter, and there are two groups of glutamate receptors, ionotropic receptors and metabotropic receptors, which are shown in Figure 1 [3]. For the ionotropic receptors, N-methyl-D-aspartate (NMDA), Alpha-amino-3-hydroxy-5-methyl-4-isoxazolepropionic acid (AMPA), and kainate receptors are included in these receptors. Experimental studies using animal epilepsy models have found that ionotropic receptor agonists induce seizure activity, but their antagonists depress seizure activity [4].

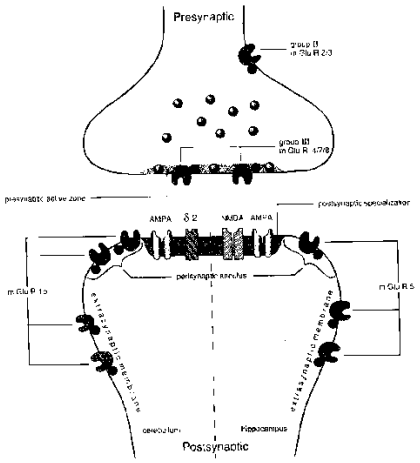

Figure 1: Diagram of various glutamate receptor and locations

2.1.3 Causes and clinical manifestations of epilepsy

Although the direct causes of epilepsy are usually not known, certain factors are known for people which will lead to epilepsy. These factors include genetic influence, brain diseases, head trauma and so on. There are some types of epilepsy and seizures that run in families. In these cases, it is more likely that there is a genetic influence. Brain diseases which will cause damage to the brain, such as brain tumors and strokes can lead to epilepsy. Head trauma, for example as a result of a car accident or some other head injuries can cause epilepsy [5].

Seizures are the main and only visible symptom of epilepsy. Seizure presentation depends on various factors, such as the location of onset in the brain, the types of seizure, the patterns of propagation, medications and so on [6]. Seizures can have an effect on sensory and motor function, consciousness, or even behavior. Seizure symptoms may include temporary confusion, uncontrolled movements of arms and legs, loss of consciousness and awareness [6]. Not all the seizures have all of the symptoms, but all seizures have a least one of them.

2.1.4 Classification of seizures

There are several different types of seizures and most seizures can be categorized as partial seizures or primary generalized seizures. Seizures that appear to involve the entire brain are called primary generalized seizures. Compared to primary generalized seizures, partial seizures originate in a specific location in the brain. There are two types of partial seizures, which are simple partial seizures and complex partial seizures. Simple partial seizures are not related to the change of consciousness, and the symptoms include for example, alterations to sense of taste or smell and dizziness. However, complex partial seizures involve a change or loss of consciousness or awareness and the symptoms include for example, staring blankly and unresponsiveness [2]. Epilepsy can be classified according to the seizure types, but also according to etiology. The classification according to etiology can be divided into genetic epilepsy, structural epilepsy and epilepsy due to unknown cause [2].

2.1.5 Epidemiology of epilepsy

Epilepsy in Europe affects around 2.6 million to 6 million people, so it represents a major concern for public health organizations and services [7]. For incidence of epilepsy, about 2-5% of the general population will suffer an epileptic seizure, however about one third of these patients will finally develop epilepsy [7]. The estimated prevalence of active epilepsy is about 3-10 per 1000, and active epilepsy is defined as a patient with epilepsy who has had at least one unprovoked seizure in the last five years. There is a large difference in prevalence between developed and developing countries, and prevalence in developing countries is much higher than developed countries because of higher rates of trauma and infectious diseases in the population [8]. The growing knowledge and technique will result in improvement in diagnostic and treatment tools, so more previously unrecognized disorders will be diagnosed

and better management of early seizures can be achieved [7].

2.1.6 Temporal lobe epilepsy

Temporal lobe epilepsy (TLE) is the most common form of complex partial seizures and the electrical abnormality originates in the temporal lobe. The complex partial seizures can evolve into secondary generalization. Temporal lobe epilepsy often appears to be because of cerebral injury at first, and after that the onset of recurrent seizures occurs after an incubation period which can be about 5 to 10 years [1].

The common symptoms of temporal lobe epilepsy include memory impairment and aura. The auras can be classified by the symptom types, which are somatosensory, autonomic and psychic auras. The auras would include a sudden sense of unprovoked fear, a sudden or strange taste [9].

2.1.7 Diagnosis of epilepsy

The diagnosis of epileptic seizures is made by analyzing the patient's detailed medical history and symptoms. There are several kinds of diagnostic methods for the patient with epilepsy involving the laboratory tests and imaging tests.

2.1.7.1 Laboratory tests

Useful laboratory tests for the patients with new onset seizures include prolactin levels to assess the etiology of a spell, and hepatic enzyme panel and toxicology screens to assess for potentially reversible causes. The lumbar puncture should be performed for the cerebral spinal fluid (CSF) examination in patient with bacterial, viral infection or other inflammatory brain disorders [10].

2.1.7.2 Imaging tests

Imaging studies must be performed to identify and classify the seizure types and etiology. Electroencephalography (EEG) plays an important role in evaluating epilepsy via sampling of electrical brain activity and it is also a common test used in diagnosing epilepsy because it is normally a noninvasive and painless test and not difficult to perform. However, EEG confirmation of seizures can be made only when a seizure is captured or identified during a routine EEG. The sensitivity of a routine EEG for epilepsy is about 50% and the specificity is about 98%, while the serial EEG can increase the sensitivity to about 80%. And then, various of activation procedures such as hyperventilation and sleep deprivation can increase the sensitivity of test. Long term video-EEG monitoring has further provided the semeiology of the seizures and it has been commonly used for seizure characterization, medication adjustment and epilepsy evaluation [11].

Neuroimaging studies are also important for the seizure and epilepsy evaluation for the determination of structural and functional etiology of seizures. 3T brain MRI is the current standard neuro-radiological imaging. Other imaging techniques are also used including

functional neuro-imaging. PET can be used to demonstrate the regional difference in metabolic activity, and SPECT can be used to analyze regional difference in blood flow during a seizure [12]. MEG and functional MRI have been found to provide more information for the localization of potential epileptogenic lesion [13].

2.1.8 Treatment options

If a patient has one single seizure, they should not be treated for epilepsy, because about 10% of people will have a single seizure during their lifetime and many of them will never develop recurrent seizures. But if a patient has at least 2 unprovoked seizures, the treatment should be performed. There are two kinds of treatments for patients with epilepsy which are pharmacological and non-pharmacological treatment and the treatment algorithm for epilepsy is shown in Figure 2 [2].

2.1.8.1 Pharmacological treatment

There are many different anti-epileptic drugs (AEDs) available, employing various of different methods to reduce the probability of having a seizure. However, there are some disadvantages of AEDs. One of disadvantages of AEDs is the common occurrence of side effects, which range from limited and tolerable side effects to dangerous side effects. Another disadvantage of AEDs is their efficacy. Although there are various types of antiepileptic medication, one third of patients with epilepsy cannot be controlled with antiepileptic medication and still suffer from refractory seizures [2].

2.1.8.2 Non-pharmacological treatment

Drug resistant epilepsy is defined as a failure of trials of two tolerated and appropriately chosen AEDs with adequate dose to achieve seizure freedom [14]. For these patients with drug resistant epilepsy, other alternative non-pharmacological treatment should be considered including epilepsy surgery and neuromodulation. Epilepsy surgery is most commonly considered if they have an identifiable epileptogenic focus which is amenable to resection and the aim is seizure freedom. Epilepsy surgery requires a presurgical evaluation to ensure that the probability of seizure freedom for the patients is as high as possible. Presurgical evaluation is based on multimodal imaging and several medical examinations to localize the epileptogenic zone. The clinical, paraclinical and imaging data can be obtained from these several medical examinations. The most important clinical data is the semeiology of the seizures, because we can get some information about the location of epileptic discharge from observing symptoms. The clinical data can be obtained by recording during video-EEG-monitoring [2]. The imaging data can be obtained from various structural or functional imaging modalities, such as MRI, PET, EEG. A neuropsychological evaluation can be used as paraclinical data [15]. When the epileptogenic zone is localized, before it is removed, it is very important to know which brain functions are localized in this zone that will be resected. Wada-test and fMRI can be used to determine the functionality of the zone.

Usually the resection will not be considered if it will cause the impairment of important and primary functions such as language, memory, etc [16].

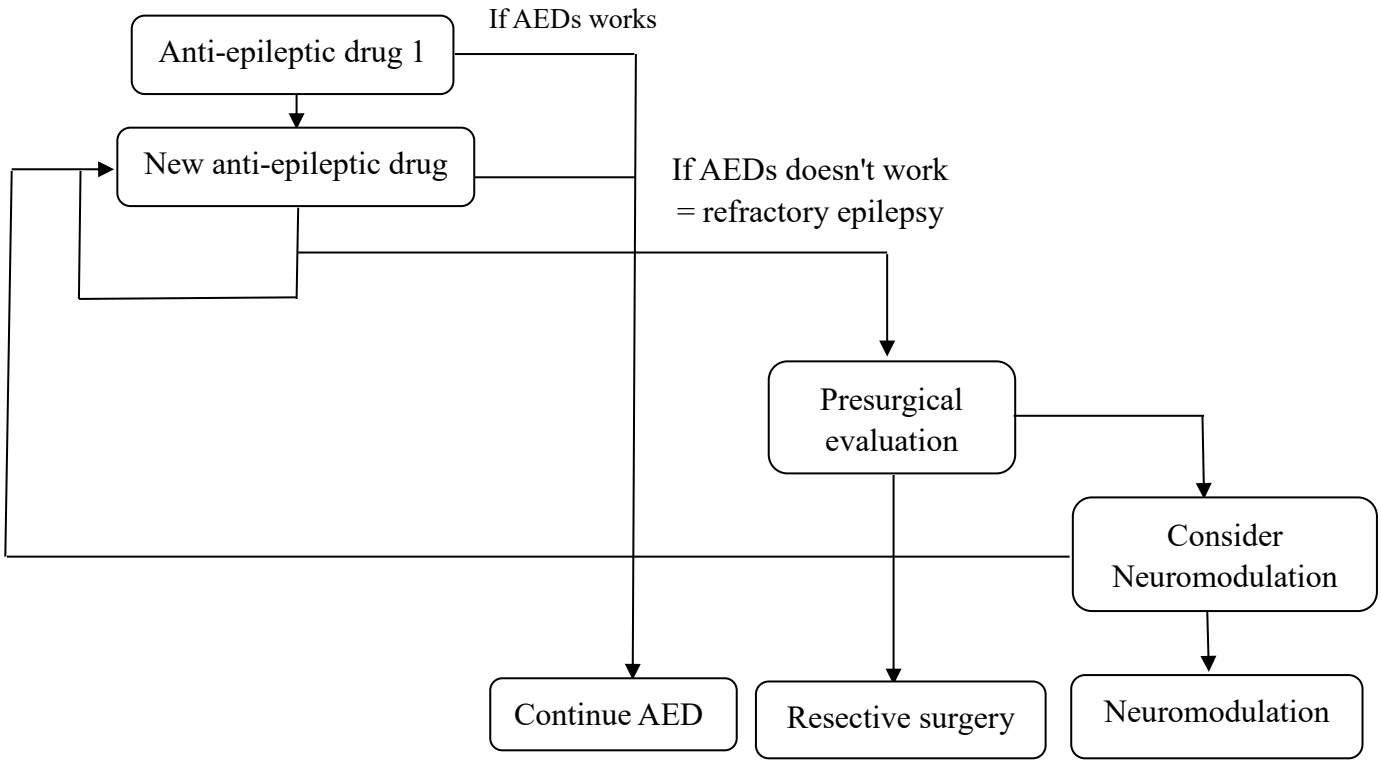

Figure 2: Treatment algorithm for epilepsy

2.1.9 Animal model of temporal lobe epilepsy

Because of the ethical and experimental limitations of human studies, detailed evaluation of underlying mechanisms of epileptogenesis and ictogenesis in patients is unfeasible, so it is very essential to make an appropriate animal model of epilepsy to investigate treatment options for epilepsy [1]. Although there is no experimental model that reproduces all the features of TLE, chronic animal models of TLE which have high level of similarity with human epilepsy have been used [17].

2.1.9.1 Kindling model

The kindling model is a commonly used model for the development of seizures and epilepsy. Increasing seizure duration and enhanced behavior of these seizures are caused by repeatedly induced seizures, and this process is called as kindling [18]. Although this model is widely used, it is controversial for its applicability to human epilepsy.

Focal electrical stimulation in the brain is the usually taken approach to carry out kindling [18]. The brains of experimental animals are stimulated with electricity or also chemicals repeatedly to induce seizures. The first stimulation produces a seizure which is quite short in duration and has small behaviors. After repeated stimulation, the length of duration and

behavior intensifies and can reach a plateau [19].

2.1.9.2 Pilocarpine model

The pilocarpine model belongs to status epilepticus (SE) models. This model appears to be highly similar to human disease, so it has been used in many laboratories since its first description. Pilocarpine is a powerful cholinergic agent and produces persistent seizures with neurodegeneration. The model is very simple to use and it doesn't require much complicated equipment. Pilocarpine is usually used for systemic administration to induce SE in rats or mice [20].

Injection of pilocarpine induces a status epilepticus and after several hours of SE, pilocarpine-treated animals recover spontaneously and they will go into a seizure-free period, which is known as latent period, before displaying spontaneous recurrent seizures which represents the chronic epileptic condition. Pilocarpine (400mg/kg, i.p) was injected in adult male rats, and a progressive evolution of seizures which is similar to kindling model, was observed [21].

2.1.9.3 Kainic acid (KA) model

Another model is kainic acid, which is a cyclic analog of L-glutamate and an agonist of ionotropic KA receptors [22]. It was isolated from the red algae (Digenea simplex) [22]. This model has been widely studied, especially in chronic epileptic state produced after a latent period following SE [1]. There are three major stages for KA model, which are the initial hours-long episode of SE, days-to-weeks long seizure free latent period, and the gradual progressive increase in the frequency of recurrent spontaneous seizures. The final stage is generally permanent and can be used to define property of chronic epilepsy.

KA can be administered in the hippocampus, intraperitoneally (IP), intravenously (IV), subcutaneously, or intracerebroventricularly. The treatments can be given as a single large dose (8-12mg/kg) or repeated lower (3-5mg/kg) doses in each hour. Our focus in this thesis is on repeated lower doses treatments because this is effective in creating an animal with chronic epilepsy.

The modeled epileptogenesis process in KA model results in similar pathological features which are commonly seen in human TLE, so it can support the validity of this model for human TLE [17].KA reproduces the seizures associated with neuronal damage which is similar with human epileptogenic tissue. It is easy to use and doesn’t require complicated equipment, except for the monitoring of EEG [17]. A main drawback of KA model is the variable sensitivity of rats of different ages, strains and weight to KA [23]. Aged rats show SE at lower dose of KA with greater neuronal damage. Another limitation of KA model is the direct excitotoxic action of KA which it makes it not easy to separate direct neuronal damage which is caused by seizures [20].

2.2 Functional magnetic resonance imaging

2.2.1 Introduction of fMRI

Functional magnetic resonance imaging (fMRI) is a technique which is used to measure brain activity according to physiological or metabolic changes in the brain. It works by detecting the changes of blood flow or blood oxygenation in the acquisition point. If one brain area is active, it would consume more oxygen with the increase in blood flow and blood volume to the active area. Because blood oxygenation changes according to the levels of neural activity, it can be used to detect brain activity. This principle is called blood oxygenation level dependent (BOLD) imaging [2]. fMRI has better spatial resolution than EEG and MEG, but the resolution is not as good as invasive procedure for example single-unit electrodes. fMRI has low temporal resolution. However, advanced techniques can improve temporal resolution, such as using multiple coils to speed up acquisition time and deciding and dropping which parts of signals matter less. It is non-invasive and safe for the subject and there is no radiation [24].

2.2.2 Magnetic resonance imaging

Magnetic resonance imaging (MRI) is a non-invasive imaging technology that produces three dimensional detailed anatomical images using a strong magnetic field and electromagnetic waves. The magnetic resonance signal from the hydrogen nuclei within water, fat or other molecules in the body can be imaged by MRI.

There are several steps to create an MRI signal. At first, when the strong magnetic field B_0 is applied, the longitudinal magnetization (M_L) would be generated, parallel to the field B_0. Then, a radiofrequency wave is applied at Larmor frequency and this would reduce longitudinal magnetization (M_L) and create a transverse magnetization (M_T). After the exciting pulse (RF), longitudinal magnetization (M_L) will recover back to its full magnitude with relaxation constant T_1 and transverse magnetization (M_T) will decay with a relaxation constant T_2. The relaxation time T_1 and T_2 are tissue dependent [25]. Because of this, the different tissues and structures can be distinguished on an MRI image. Tissues with a long T_1 appear dark and tissues with a short T_1 appear bright on a T1 weighted image. Fat will show up the brightest, so the white matter would be brighter than gray matter and cerebral spinal fluid will be dark. An example of T_1-relaxation curves and a corresponding T1 weighted MRI image are shown in Figure 3 [2]. Another example of T_2-relaxation curves and corresponding T2 weighted MRI image are shown in Figure 4. In this case, water or cerebral spinal fluid will be brightest and white matter would be darker than gray matter. Because of field inhomogeneities, T_2will often be replaced by T_2^* in reality.

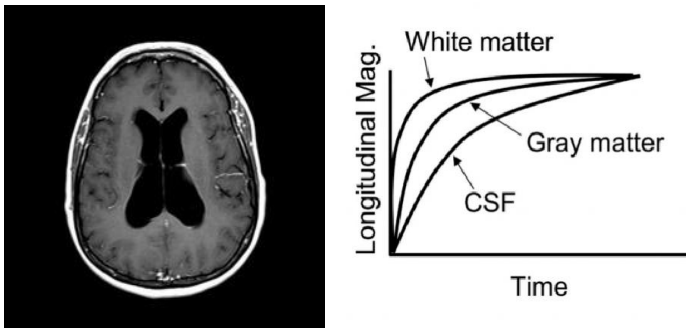

Figure 3: T_1-weighted image and T_1-relaxation curve [2]

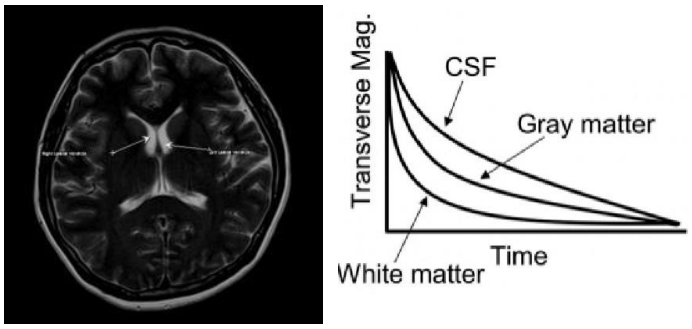

Figure 4: T_2-weighted image and T_2-relaxation curve [2]

An MRI sequence is an ordered combination of RF and excitation pulses designed to acquire the data to form the image. Each excitation pulse is separated by a repetition time TR. Data is measured at some characteristic time after the application of excitation pulses and this is defined as the echo time TE [26]. The spin echo (SE) sequence is commonly used, shown in Figure 5. The spin echo (SE) sequence starts by switching on the slice select gradient (Gss), and this gradient is used to select the slice from which the signal will be sampled. The $90°$RF excitation pulse is applied at the same time. Then the phase encoding gradient (Gpe) and read out gradient (Gro) are switched on to know the location of the image voxels [27]. The refocusing of the spins is obtained by applying a $180°$RF pulse after the $90°$RF excitation pulse. The signal will increase again after the $180°$RF pulse, and this is called the echo. This $180°$pulse is applied exactly halfway between the excitation pulse and the echo.

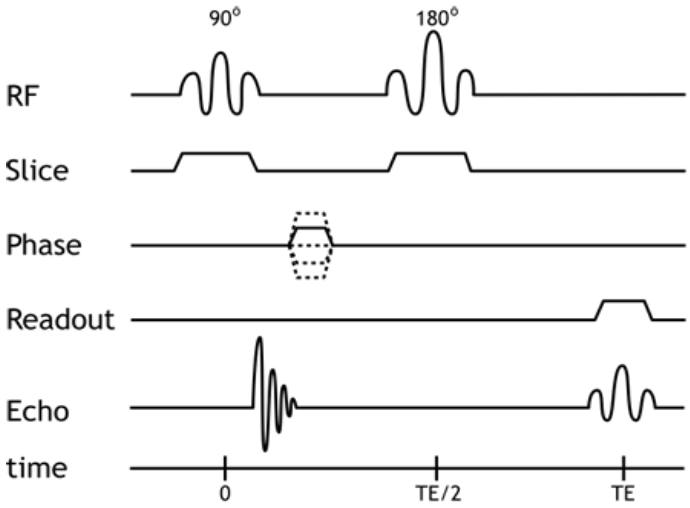

Figure 5: Diagram of SE sequence

Another sequence is the gradient echo (GE) sequence, shown in the Figure 6 below. Because a 90°RF excitation pulse is always used in a SE sequence, T_1 relaxation can take a long time. It can be avoided by using gradient echo (GE) sequence. GE sequence uses gradients with opposite signs to dephase and rephase the spins. 180° RF pulse is not used in GE sequence, allowing lower flip angles for RF excitation. The signal is obtained during the Readout gradient (Gro), and by changing the polarity of the Readout gradient, the same effect can be obtained as by applying a 180°pulse RF-pulse.

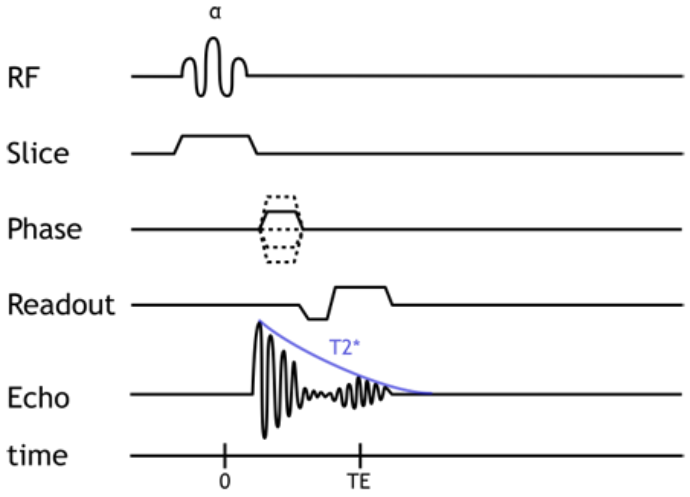

Figure 6: Diagram of SE sequence

2.2.3 fMRI principles

Blood oxygenation level dependent (BOLD) fMRI is the most often used technique in fMRI. So the blood oxygenation level can be used to detect brain activity [2]. When a brain area is activated, the neurons become hyperpolarized and to get them back to their polarized state requires actively transporting ions across cell membranes, so ATP is needed during this transport process. Glucose is the brain's primary energy source and ATP can be formed from

oxidizing glucose, but glucose is not stored in the brain [28]. If the brain activity increases, more ATP is needed and more glucose is required, so the blood flow to the active area will increase to transport more glucose. And more oxygenated hemoglobin molecules are brought in red blood cells with the transport of more glucose [29].

Oxygenated hemoglobin (oxyHb) is diamagnetic while deoxygenated hemoglobin (deoxyHb) is paramagnetic. Deoxygenated hemoglobin has a paramagnetic moment so there is a local disturbance of the magnetic field, resulting in a shortening of the T_2^*- relaxation time of the tissue so there is a loss of MRI signal compared to tissue with oxyHb [30].

When brain neurons in a region are activated, and the cerebral metabolic rate for O_2 has increased, there will be less oxygenated hemoglobin and more deoxygenated hemoglobin in this active region. However, blood flow and blood volume are also increased, leading to a high increase of oxygenated hemoglobin and a decrease of deoxygenated hemoglobin. This is shown in Figure 7 [2]. The increase of blood flow and blood volume are much higher than the oxygen metabolism, so the total amount of oxygenated hemoglobin will increase and deoxygenated hemoglobin will decrease. So the BOLD signal, which is the ratio of oxygenated hemoglobin to deoxygenated hemoglobin, increases and the T_2^* weighted MRI signal increases. Therefore, the active areas in the brain appear to be brighter than other regions on a T_2^*-weighted image [2].

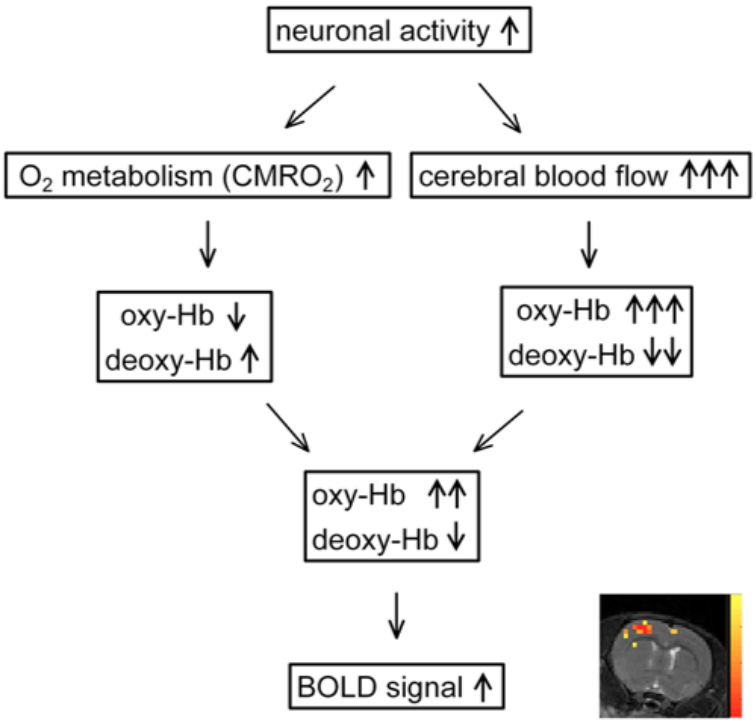

Figure 7: BOLD signal is the combination of the effects of oxygen metabolism and blood flow [2]

2.2.4 Hemodynamic Response Function

BOLD fMRI allows us to study the hemodynamic responses to neural firing. The change in the MRI signal which is caused by a neural event is referred to as the hemodynamic response function (HRF), and it is shown in Figure 8. There is a decrease in blood oxygenation after the neurons are active, which is known as the initial dip in the hemodynamic response. At this time, the metabolic demands increase due to the neuronal activity and it leads to an increase in the flow of oxygenated blood to active regions of brain. Because more oxygen is supplied than demanded, this leads to a decrease in the deoxygenated hemoglobin, which leads to an increase in signal following neural activation. The positive increase in the signal starts 1-2 seconds after the initial dip and peaks after about 6 seconds after peak neural activity. After the peak level, the BOLD signal decreases below baseline level, often followed by a positive-stimulus undershoot [31]. Since the blood flow decreases more rapidly than blood volume, so there is more deoxygenated hemoglobin present.

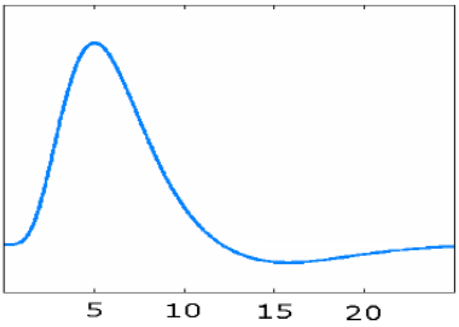

Figure 8: Hemodynamic response function

2.2.5 Echo Planar Imaging

Echo planar imaging (EPI) is a fast MR image acquisition technique and it is used to acquire brain images, every few seconds, during several minutes. EPI is so fast because it can acquire all frequency and phase encoding points in one single pulse cycle. It is called "single-shot" because it can collect the entire 2D image in one TR.

Spin echo and gradient echo can be used to offer a wide range of contrast behaviors. Figure 9 shows the most common implementation of EPI which is used for clinical imaging: the spin echo sequence [32]. The phase and frequency encoding is preceded by an 90°excitation pulse and 180°echo-forming pulse, and an echo can be formed during readout period. For Gradient Echo (GE) sequence, EPI data collection follows a single RF pulse, with a flip angle between1°to180°, depending on the preferred contrast. This is shown in Figure 10 [32].

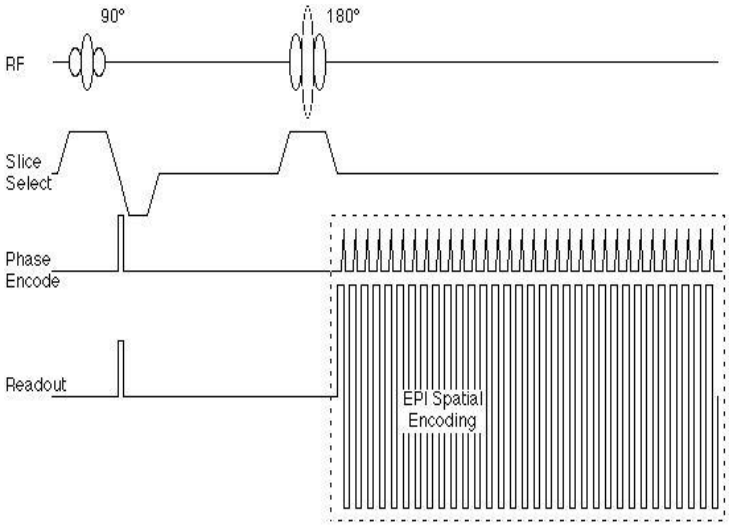

Figure 9: Echo-Planar pulse sequence

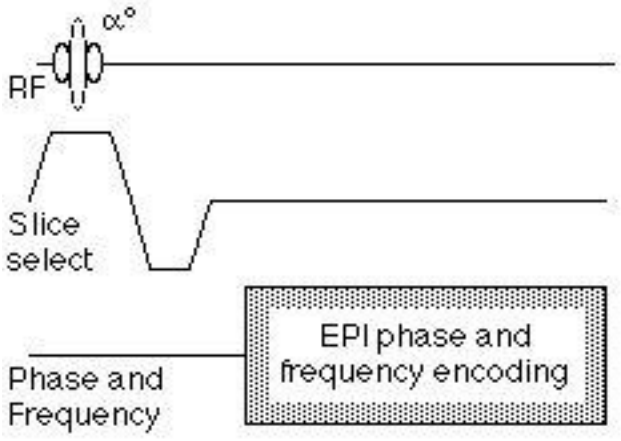

Figure 10: Gradient Echo EPI sequence

2.2.6 fMRI paradigm design

The stimulus should be given to the region of interest in order to measure the brain activity or visualize the certain brain regions. The meaning of 'paradigm' or 'design' is the way how tasks and stimuli are organized [33]. The most common used designs are the block design and event-related design. They are shown in Figure 11 [33]. In a block design, stimuli are presented within one condition and alternate this with other moments when a different condition is presented. Individual hemodynamic response functions from each stimulus can be combined in BOLD response, so the BOLD response has higher magnitude. Therefore, it is best for detect differences in BOLD signals between conditions, however it is not good at isolating different responses to single event within the block.

Another common used type of design is the event-related design. It can enable us to design more complex experiments. Hemodynamic response function for each individual event can be detected when very short stimuli are given. It is best for estimating the shape of response function and looking for the differences in timing. Compared with block design, the

resulting curve of event-related design depends on the shape of impulse response [33].

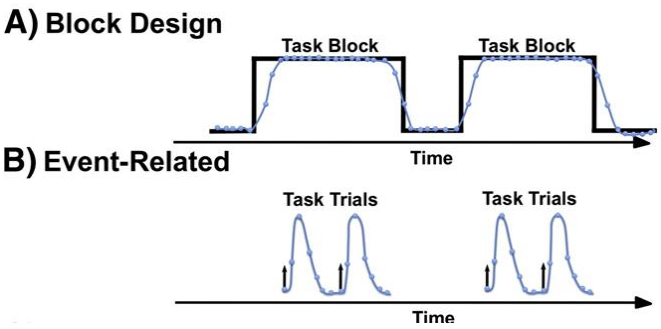

Figure 11: A: Block design, B: Event-related design

2.2.7 Resting state fMRI

Much of what we previously knew about the brain comes from the research of task-related fMRI during which a stimulus is applied. In recent years, another method called resting state fMRI has been used to examine the functional organization of brain. In resting state fMRI the brain is imaged during rest state when no external stimulus is applied. The resting brain activity can be observed by the BOLD effect because any brain regions have spontaneous fluctuations in the BOLD signal when there is not an external stimulus or task [2]. The goal of the resting state method is to find out the functional organization of the brain and compare the difference in signal between healthy subjects and subjects with neurological or psychiatric diseases. Also, a number of networks have been found in healthy or abnormal subjects, different stages of consciousness and across species. In particular it has been shown that fluctuations in the low frequency part of the BOLD signal show strong correlations across distant regions. Temporal correlation between different regions in the network can be calculated based on the time course of the signal and also functional connectivity can be derived from this [2].

Resting state fMRI is based on the study of low frequency BOLD fluctuations and the oscillation frequency of spontaneous BOLD can be easily separable from frequencies of respiratory and cardiovascular signals [34]. Typical resting experiments are about 5-10 min, and there is no consensus whether the data should be collected while the subjects are awake. Preprocessing steps of resting state fMRI normally follows the same principles which are applied to standard task-related fMRI. However, the data is band-pass filtered at 0.01-0.1 Hz because of the interference of these non-neuronal physiological signals which are mentioned before, instead of high pass filtering which is applied to task fMRI data because it would remove some useful information. In addition, the cerebrospinal fluid (CSF), and the white matter are commonly removed before analysis to reduce the effect of head motion [34].

Due to the lack of task and stimulus, resting state fMRI is attractive because it removes the burden of experiment design, subject compliance and training demands of the subjects. Also, it is easy to complete a resting state scan when performing task-based experiments.

Because of these reasons, it is commonly used and attractive in the studies of clinical population [35].

2.2.8 Applications of fMRI

Functional MRI has a small but growing role in clinical neuroimaging and also there are some initial applications to neurosurgical planning.

2.2.8.1 fMRI guided neurosurgery

fMRI can be used for pre-surgical mapping to localize cerebral function in tissue within or near regions which are intended for neurosurgical resection [36]. fMRI is necessary for precise and safe neurosurgical planning.

2.2.8.2 Parkinson's disease

Functional imaging can not only study the process underlying Parkinson's disease (PD) symptoms, but also can be used to detect the subclinical and early disease and monitoring the progression of disease [37]. fMRI can be applied to investigate cognitive disturbances in patient with PD [38]. The studies about motor activation can be completed by quantifying BOLD signal changes during the performance of a task. Therefore, the changes of activation patterns which are characteristic for PD can be identified [38]. Resting-state fMRI can be used to gain more information about pathophysiology of PD and it can assess the functional abnormalities without the effect of a specific cognitive task. By using this kind of method, it might be possible to separate patients with PD from healthy people, so fMRI can be used as a diagnostic tool for PD.

2.2.8.3 Epilepsy

Many diagnostic methods have been used for the presurgical evaluation and management of epilepsy, including the intracarotid amobarbital testing (IAT) or Wada test, regarded as the golden standard for a long time [39]. The Wada test is performed during angiography and it can identify the side of brain which controls language and show the area of memory function in the brain. Functional MRI (fMRI) is also a promising tool for the management of epilepsy and it can provide a less invasive alternative to the IAT [39]. Also, by mapping the eloquent area with fMRI, it can be used to predict and manage the possible deficits in motor and sensory or language functions which could be caused by surgery [39]. Lateralization of language and memory function can be identified with fMRI. EEG and fMRI can be integrated to localize the changes in regional brain activity. The combination of EEG and fMRI can utilize the high temporal resolution of EEG and high spatial resolution of fMRI to aid in seizure localization.

2.2.8.4 Migraine

Migraine is a common neurological disorder which is characterized by headache [40]. A non-invasive approach based on kinetic oscillatory stimulation (KOS) for the treatment of migraine has been developed [41]. By using the blood oxygen-level dependent (BOLD)

functional MRI, the alterations in the functional connectivity in the brain which are responded to KOS treatment can be studied [41]. So by comparing the resting state functional connectivity differences between patients with migraine and normal volunteers before and after KOS treatment, it is demonstrated that migraine is related to abnormal functional connectivity in the limbic systems. And KOS treatment can regulate this abnormal status in limbic systems back to normal status.

2.2.9 Preclinical Imaging

Imaging has become very important in clinical practice and preclinical imaging is the bridge between the molecular and clinical imaging.

2.2.9.1 Preclinical imaging

Small animal imaging has become a critical part of preclinical biomedical research. Because the volume and size of small animals (rats or mice) is much smaller than human body, the spatial resolution of small animal imaging should be about 10 times smaller than human imaging. The signal of small animal imaging would be much smaller than human imaging so there should be some refinements of these imaging modalities [42]. For micro-fMRI, small animal imaging should be conducted at higher field strengths, and also the gradient fields and coils should be improved. To obtain the high spatial resolution data, the acquisition time is really long and it can even extend to one hour, so this is one drawback of micro-fMRI. Another disadvantage is the large cost of the facility .

2.2.9.2 Anesthesia

The main challenge for preclinical imaging is the biological motion not only the physical motion of small animal, but also the respiratory and cardiac activities affecting the quality of images. Compared with human studies, a specific requirement for small animal imaging is anesthesia which helps to restrain and immobilize the animal. But the cardiac and respiratory motion still should be considered to be controlled [43].

The handling and preparation of animals and the anesthesia regimes are the challenges when carrying out functional MRI. Since physiological parameters can influence fMRI signal, it is very important to keep these parameters stable to allow for the detection of a physiological response related to the stimulus. A MRI-compatible system which includes ECG, temperature, blood pressure and respiratory monitoring equipment is used to test and monitor these physiological parameters [43]. Respiration is the only physiological parameter we monitored in this master thesis.

Injectable and inhalation anesthesia methods are commonly used in rats [43]. Inhaled anesthetics have rapid onset and recovery times, it is easier to control the doses and maintenance time of anesthesia, so they are more suitable for imaging. The injectable agents

need to be metabolized by the liver and excreted by the kidney, whereas the inhaled agents will be eliminated via the lung quickly [43].

Inhalation anesthetics Inhaled anesthetics are not stable compounds which have a specific effect on the central nervous system. The inhalation anesthesia must produce complete anesthesia, the induction and recovery should be rapid, and they have to be safe, non-irritant and non-explosive. Isoflurane and halothane are the most commonly used inhalation anesthetics. Isoflurane is widely used because it is minimally metabolized by the liver and is less toxic than injectable anesthetics. An overdose can be fatal, so animals should be induced individually and then the maintenance percentage has to be reduced when the animals are unconscious. Isoflurane has become a better agent for cardiovascular studies because it depresses cardiac function less than injectable anesthetics. However, it causes a decrease in blood pressure by reducing peripheral resistance.

Injectable anesthetics For injectable anesthetics, the anesthetic dose rates for injectable agents will depend on various factors which are the type of species, the administration of age, sex, body condition and the level of anesthesia required. Three injectable agents that are often used are medetomidine, ketamine and Fentanyl.

Medetomidine Medetomidine is commonly used in fMRI studies for small animals and its active enantiomer, dexmedetomidine, is used in human medicine. Medetomidine has many beneficial effects on anesthesia practice, including reliable sedation (not being under full anesthesia), analgesia, muscle relaxation and anxiolysis [44]. Medetomidine exhibits a rapid distribution, on the order of minutes, to the brain, so it leads to a good control of the depth of anesthesia. Medetomidine has an influence on vascular responses resulting in the decrease of CBF and CBV. But the dose-dependent effect of medetomidine on functional BOLD response has not been evaluated systematically. Medetomidine is a perfect anesthetic to use when we want to study the relation between neuronal activation and the hemodynamic properties of the BOLD signal in fMRI experiment. A reasonable time window for BOLD-fMRI responses is 1-2 hours when a constant infusion rate is used. And it is also found that a constant infusion of medetomidine at 100μg/kg/hr is not enough to maintain sedation beyond 3 hours, so it is necessary to increase the infusion dose after 3 hours.

Ketamine Ketamine is an anesthetic which is commonly used in the veterinary field. It can produce a state in which there is profound analgesia, light sedation and muscle rigidity [45]. And it doesn't depress central nerve system, so reflexes remain intact. But there are some negative effects of ketamine and one of the negative effects is the eyes of animals remain open, so the ophthalmic ointment is required and the spontaneous movements and muscles cause an initial increase in blood pressure. Compared to other anesthetics, ketamine doesn't depress the cardiac and respiration output. Ketamine cannot achieve the surgical anesthesia on its own, so it is often used in combination with xylazine, medetomidine during surgery.

Fentanyl Fentanyl is licensed for sedation in rodents, rabbits and pigs. Because of its poor production of muscle relaxation, it cannot be used on its own for surgery [43]. So it should be used in combination with benzodiazepine (midazolam or diazepam) for surgical anesthesia in rodents, rabbits and pigs because it will produce good muscle relaxation [43].

2.2.10 Limitations of fMRI

fMRI doesn't measure neural activity directly, but shows the changes in blood flow and volume caused by the modulation in neural activity. The researchers still don't completely understand the relation between fMRI measurements and neural activity. The fMRI can't convey the detailed information about the activities of individual neurons, which are very important to mental function of brain. Each area of brain studied in fMRI is made up of many individual neurons, and each of them may have different functions [46]. If the certain areas of brain which "light up" on fMRI may represent different functions, it is really hard to tell exactly what kind of brain activity is being represented on the scan.

Another significant limitation of fMRI is its low temporal resolution because the BOLD contrast is derived from delayed hemodynamic response to metabolic changes. Also, because the change of deoxygenated hemoglobin concentration in the blood often occurs further away from the activated neurons, it is imprecise to locate the activation area [47].

2.3 Dynamic functional connectivity

Functional connectivity is defined as the study of temporal correlations or dependency among two or more anatomically distinct neurophysiological events. Until now, most fMRI studies have assumed that the functional connectivity of signals between distinct brain regions is constant throughout the recording periods [48]. It is referred as static functional connectivity (sFC). More recently, temporal fluctuations in functional connectivity within the session have been found, and it is referred to as dynamic functional connectivity (dFC).

2.3.1 Static functional connectivity (sFC)

The most well-known functional connectivity measure is the correlation, which is called the Pearson correlation coefficient. It calculates the linear relation between the two signals based on the amplitudes of the signals. Another measure is cross-correlation which investigates the correlation between two signals in function of time and they are shifted in time with respect to each other. In the frequency domain, the counterpart of cross-correlation is coherency [2].

Correlation coefficient

The correlation coefficient (ρ_{xy}) is a simple connectivity method to assess the interdependency between two time series (x and y). The formula to calculate the correlation coefficient is shown as follows [2]:

$$\rho_{xy} = \frac{E[(x-\mu_x)(y-\mu_y)]}{\sigma_x \sigma_y} = \frac{1}{N}\sum_{n=1}^{N} \frac{(x(n)-\mu_x)(y(n)-\mu_y)}{\sigma_x \sigma_y}$$

Where N is the number of samples, E[x] is the expected value of x, μ_x and μ_y are the mean values, and σ_x and σ_y are the standard deviations of the signals. The correlation coefficient lies between -1 and +1. Negative values represent negative correlation and positive value indicates positive correlation and 0 means there is no correlation.

Cross-correlation

The cross-correlation estimates the correlation between two time series that are shifted in time, which is shown as follow:

$$\rho_{xy}(\tau) = \frac{E[(x_n-\mu_x)(y_{n+\tau}-\mu_y)]}{\sigma_x \sigma_y} = \frac{1}{N-\tau}\sum_{n=1}^{N-\tau} \frac{(x(n)-\mu_x)(y(n+\tau)-\mu_y)}{\sigma_x \sigma_y}$$

Where τ is time lag which represents how much y shifted with respect to x, and it can be used to assess the directionality of the correlation.

Correlation matrix

Correlation coefficient can be calculated to evaluate the association between two or more variables. Correlation matrix can be used to investigate the dependence between multiple variables at the same time. The correlation matrix can be seen as a table containing the correlation coefficients between each variable and the others.

2.3.2 Dynamic functional connectivity (dFC)

In recent years, FC has been shown to fluctuate over time, so there has been a shift from static analysis of functional connectivity to dynamic functional connectivity (dFC), because dynamic properties of the BOLD signal fluctuations have been found.

There are various of analysis methods for dynamic functional connectivity. The most common and straightforward method to investigate dFC is using sliding windowed FC, which was first introduced by Sakoglu and Calhoun in 2009, and applied to schizophrenia [49].

2.3.3 Dynamic functional connectivity analysis

2.3.3.1 Independent component analysis (ICA)

Independent component analysis is a computational and statistical technique for separating signals into different subcomponents in signal processing field. This is done by

assuming that all the subcomponents are statistically independent from each other. Normal independent component analysis provides only steady-state information of the networks over the scan time and the relationship between different areas involved in the network is assumed to be kept over the entire scan. Therefore, this kind of analysis method cannot give any information about spatiotemporal dynamic changes of the signal.

Spatial ICA (sICA) has been applied to fMRI as a data-driven method and it can estimate the network from the entire spatiotemporal dataset at one time. This is one method to apply the degree of variability into ICA FC estimation by performing sICA on a sliding-window basis [50]. The functional connectivity profile of default mode network was found to vary over sliding windows.

2.3.3.2 Sliding window technique

Sliding window analysis is performed by conducting analysis on a set number of scans within fMRI sessions. To complete the sliding window step, optimal window length and step length should be determined at first. The correlation coefficients between different ROIs are calculated over consecutive windowed segments of data. The defined window is then moved forward in time. A time series of FC values can be obtained and they can be used to assess fluctuations in FC within sessions. One benefit of this sliding window analysis is that almost steady state analysis can be performed if the window length is large enough.

The following description is dFC analysis using sliding window approach. Instead of calculating the Pearson correlation using the whole activity time course across, dFC is based on the segmentation of the activity time course. The window ‘w’ segments the whole activity time courses into more or less overlapping parts. After segmenting the activity time courses, correlation coefficient will be calculated for each window segment. We can see from the Figure 12 [51] that sliding window method is applied and for each window, the data points within this window are used to calculate correlation matrix. The window is shifted in time by a step length which defines the overlap between two windows, and we can obtain a series of correlation matrices. From the results, we can indentify that correlation matrices vary over time.

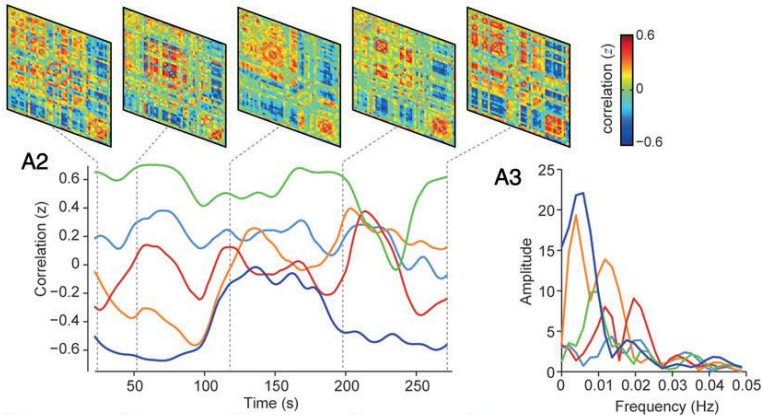

Figure 12: The figure ([51]) shows the temporal evolution of functional connectivity

2.3.3.3 Clustering analysis

K-means algorithm is one of the common unsupervised learning algorithms which solve all the well-known clustering problems. The procedure follows a simple and easy way to classify a given data through a certain number of clusters (k clusters). The main idea of this algorithm is to define k centroids, one for each cluster. And then we need to put them as far from each other as possible. In the next step, each point should be taken belonging to a given data set and associated the nearest centroid. When all the points have been taken, early groupage is done. At this point, we need to calculate k new centroids as the barycenters of the clusters from previous step. When we obtain k new centroids, a new association has to be done between the data points and nearest new centroid, so the loop of this algorithm has been generated. The location of k centroids will change their location step by step until there is no more changes of their location. The aim of this algorithm is to minimize the objective function, which is shown as follow [52]:

$$\mathrm{J} = \sum_{j=1}^{k} \sum_{i=1}^{n} \left\| x_i^{(j)} - c_j \right\|^2$$

Where $\left\| x_i^{(j)} - c_j \right\|^2$ is the distance measured between a data point $x_i^{(j)}$ and the cluster center c_j.

To assess the frequency and structure of dFC connectivity patterns, the k-means algorithm can be used to cluster these dynamic functional connectivity windows, partitioning the data into a set of separate clusters in order to maximize the correlation within a cluster to cluster centroid. The initial clustering was performed on a subset of windows from each subject, instead of clustering all of dFC windows across all the subjects. The subset of windows from each subject can be obtained by selecting windows corresponding to local maxima after we have calculated the variance of dFC across all parts at each window. The optimal number of centroids can be estimated using the elbow criterion, defined as the ratio of

within cluster to between cluster distances. These sets of initial groups of centroids were the starting point to cluster all the dFC windows across all the subjects.

2.3.4 Applications of dFC

There are some clinical applications for the analysis of functional connectivity. Physiological diseases have disrupted large-scale functional or structural properties. Quantification of disrupted dynamics in clinical populations may lead to a better understanding of disease and targeted drug treatment. Therefore, an improved understanding of the relation between disease and dynamics can enhance the understanding of how dynamic functional connectivity properties support brain function. Altered dynamics in schizophrenia, depression and Alzheimer's disease have been examined to find the link between disease and dynamics.

2.3.4.1 Schizophrenia

Sensory, motor and frontal networks had less engagement with other networks and there is a significant difference in time-frequency patterns of connectivity between schizophrenic patients compared to healthy controls. And the FC window states switch more often in healthy controls, while patients with schizophrenia tend to have a state of "weak" and relatively "rigid" connectivity. This finding cannot be detected using a static FC method [49].

2.3.4.2 Depression

The transition of FC as a marker of dynamic brain state changes can be well corresponded to current findings of brain activity in depression. Major depressive disorder (MDD) is a recently proposed model and it suggests alterations in static FC could be due to bias toward more frequent down states and it would predict a decrease in mood-related brain dynamics [53]. Initial findings have supported the notion that the resting-state dynamics of key structures in MDD may be altered and it provides the correlation with the subject's decreased ability to react to external and internal cognitive demands [53]. More work is needed to understand connections between brain network dynamics and changing affective states.

2.3.4.3 Alzheimer's disease

Previous studies have found altered static FC measures in Alzheimer's patients compared with healthy controls. Also, the author reported differences in the "dwell time" within different sub-network configurations of the default-mode network (DMN) between Alzheimer's patients and old healthy controls [54]. More specifically, there was less time spent in brain states with stronger posterior DMN region contributions [54]. It can provide a

more accurate description of Alzheimer's disease and lead to a better understanding of the characteristics of the disease and better diagnostic indicators.

2.3.5 Limitations of dFC

There are some limitations for using dFC. First, our ability to make the conclusions from dFC and states is limited. Because of uncontrolled nature of the resting-state scan, we have few tools to investigate changes in FC, and the functional roles of dynamics and the relations to cognitive states remain unknown. Then, the most common limitation is that of overlooking the fact that the observed FC values are estimates of the true and not observable values, and hence, there is some statistical uncertainty [55]. Although the fluctuations are real, the observed dynamics may be driven by time-varying noise and don't reflect fluctuations in BOLD signals. Noise in the fMRI can arise from a various of factors including the heart beats, changes in blood brain barrier, characteristics of the acquiring scanner. The noise cannot be completely eliminated with most preprocessing techniques. An appropriate statistical test has to be done to decide whether the fluctuations are due to statistical uncertainty or true changes in population FC. Another experimental limitation of the study is the limited data available for each subject. Each subject was scanned for a short time, and the dynamics of the connectivity and state transitions at the level of the individual can not be precluded. Therefore, longer scanning time can improve the estimation of dFC variability and permit patterns of connectivity to reoccur several times within the scanning time and this is important for future investigation [51].

Chapter 3 Materials and Methods

3.1 Kainic acid (KA) rat model

In this experiment 12 adult male Sprague-Dawley rats (0.276± 0.019 body weight; Envigo, Netherlands) are used. In this part, intraperitoneal kainic acid (IPKA) rat model was used to obtain epilepsy rats.

KA can be administered by many methods which are described in literature overview part in this paper, and IPKA rat model was used in this master thesis. KA injection according to the Hellier protocol [1], resulted in chronic epilepsy in all rats.

In the Hellier's study [1], they have tested the hypothesis that rats receiving multiple low-dose systemic injections of kainate (i.e. 5mg/kg per h) chronically develop seizure characteristics which are similar to those of human temporal lobe epilepsy. This kind of modified kainate treatment protocol (i.e. repeated low-dose injections of kainate) has a greater efficiency compared to other protocols, because the injections are performed intraperitoneally and the exposure to kainate is extended. Repeated low dose intraperitoneal (i.p.) injections of kainate can reduce the mortality rate and allows slower diffusion to the brain compared to other injection methods, and it is effective in creating an animal with chronic epilepsy.

Kainate (5mg/kg) was administered to six healthy male Sprague-Dawley rats intraperitoneally every hour until the animals displayed a stable status epilepticus (SE) for three hours, and control rats were treated similarity with saline [17]. Seizures were determined by observing the behavioral postures.

3.2 Image acquisition

3.2.1 Anesthesia

The rat was anesthetized with 5% isoflurane mixed with 1.5L/min oxygen. And after this period, isoflurane was reduced to 2% mixed with 0.3L/min oxygen for maintenance during preparation for imaging. Then the neck of the rat was shaved and the needle (30G) was inserted under the skin for subcutaneous infusion of medetomidine. And next, the rat was placed on a heated water pad while in the magnet to maintain the temperature. A pressure sensor placed under the chest was used to continuously monitor breathing. After this step, the rat was given a bolus of medetomidine (0.05mg/kg) and after 10 minutes isoflurane was discontinued. Anesthesia was maintained with a constant medetomidine infusion rate (0.1mg/kg/h). The timeline of anesthesia protocol can be seen in Figure 13. After the image acquisition step, the anesthesia can be reversed with atipamezole.

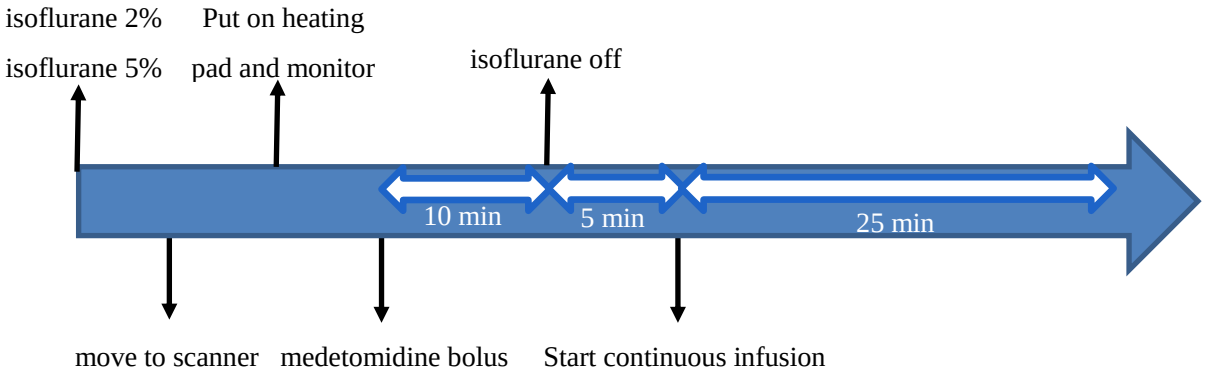

Figure 13: Timeline of anesthesia protocol

3.2.2 Functional MRI acquisition

In this master thesis, functional MRI is the only imaging modality for preclinical research, and it allows longitudinal non-invasive serial imaging studies within the same animals.

The resting-state fMRI images were acquired with a Pharmascan 7T (Bruker). Firstly, a wobble was done to match and tune radiofrequency coil. Then a tripilot scan was performed to get the information about the position of animal in the scanner. The magnetic field homogeneity can be improved by shimming. One TurboRARE T2 image of each rat was acquired after shimming. This kind of anatomical image has a better resolution than functional images and can be used to localize different brain regions of interest more accurately. After that, the functional MRI images were acquired.

About 30 minutes after turning off isoflurane, the resting-state fMRI images acquisition is performed using a standard gradient-echo echo planar imaging (EPI), with TR=2s, FOV=0.375mm, slice thickness/gap=1mm/0.1mm, scan matrix=80×80. This EPI imaging run is repeated 300 times in ten minutes and we can obtain 3 rsfMRI images.

3.3 Data analysis

Different analysis techniques and software are used to analyze fMRI images: statistical parametric mapping package (SPM12 [56]), sliding window technique with the toolbox GRETNA [57] and k-means clustering performed by a script written in Matlab. When the original resting-state fMRI images are obtained, the images will be preprocessed firstly. Then the sliding window technique is performed of these preprocessed images. After this, all the correlation matrices are divided by k-means clustering method. And finally, the results of these clustered matrices are used to perform necessary statistical analysis to compare the epileptic and healthy rats and obtain the conclusion.

3.3.1 Preprocessing steps

Preprocessing is necessary in fMRI analysis in order to prepare raw data from the scanner for statistical analysis [58]. Therefore, before fMRI data can be analyzed, several preprocessing steps need to be completed. The fMRI images are preprocessed using SPM12. Firstly, slice timing correction can be performed to adjust and correct for the time difference between different slices of the brain. Then, the different images have to be realigned to correct the data for the effects of movement during the scanning period. And next, the structural image is superimposed on a functional image to localize and visualize the active brain areas better in the coregistration step. After this step, the normalization step needs to be completed to normalize functional image to EPI template. In addition, the functional images are spatially smoothed with Gaussian filter to increase signal to noise ratio [59]. In the last step, the bandpass filter is used to remove all non-neurological signals. The flow chart of all the preprocessing steps is shown in Figure 14.

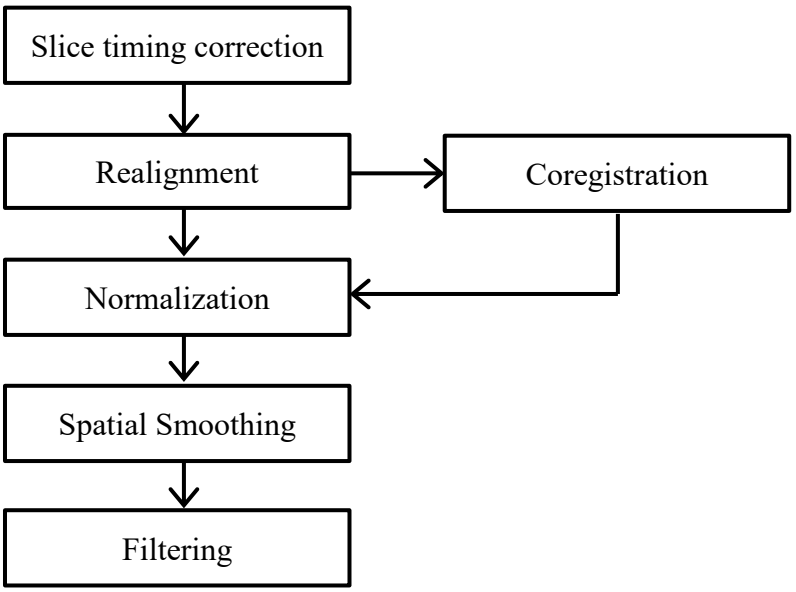

Figure 14: Flow chart of all preprocessing steps

3.3.1.1 Slice timing correction

When individual slices are recorded, there is a time difference to acquire different slices. Therefore, it is not correct to assume that all the slices were acquired at the same time [58]. This can be done by using temporal interpolation of the slices with respect to the reference slice to make it appear as though all of the slices were acquired at the same time.

In the slice timing correction step in SPM12, several parameters have to be chosen. For each subject, three sessions are added, each contains a time series of images (300 images). The parameters of slice timing correction in SPM12 which are chosen for our experiment are the number of slices of 16 and TA (acquisition time) of 1.875s. The other input parameters

which need to be changed are slice order, TR, and reference slice. The slice timing order of acquisition we chose is interleave model which is odd numbered slices acquired then even numbered slices, and the order of slice acquisition determines when in hemodynamic response the signal for a slice is acquired. The repetition time (TR) is set to 2s and the reference slice is the eighth slice.

3.3.1.2 Realignment

In the reality of the experiment, the subjects cannot lie perfectly still in the scanner while the experiment is completed on them. Therefore, different images have to be realigned with a motion correction algorithm to correct the data and remove the effects of movement during scanning period [59].

In the realignment step in SPM12, there are some parameters which need to be chosen. For each subject, three sessions after the slice timing correction are added. The standard parameters in this step which need to be changed are the separation of 0.4mm and the smoothing (FWHM) of 0.5mm. A mean image is created at one time point and the realignment is done for each time series separately.

3.3.1.3 Coregistration

The anatomical or structural images have a higher spatial resolution compared with functional images. The structural images can be superimposed on a functional image to visualize and localize active brain regions better. The structural image and functional image have different acquisition parameters, so they have to be coregistered first. During the coregistration step, the T2 image, which can be seen as structural image, is registered to the mean of three EPI images.

The difference of the parameters in this step compared to realignment step is the parameters are estimated with another objective function, which is normalized mutual information.

3.3.1.4 Normalization

There are large variations between individual brains, and even major landmarks such central sulcus will vary in different subjects' brains, considering the position and length. Although the brains of Sprague-Dawley rats are more similar than humans, it is also necessary to complete normalization step for preprocessing the images. Spatial normalization can wrap individual brains into a common reference space and it allows the fMRI signal changes across individuals within a group of subjects. An EPI template is necessary to achieve the normalization of the mean EPI image, and mean EPI image can be normalized to EPI template. Except for the EPI template image, a template weighting image is also important for this normalization step. The template weighting image is a mask for

normalization of KA rat images.

3.3.1.5 Smoothing

Smoothing can increase the ability to detect task-related signal changes and the signal to noise ratio at the cost of reduced spatial resolution [58]. In this step, a spatial Gaussian filter is applied to the images. The size of 3D Gaussian kernel is at least twice of the voxel size. Smoothing can be seen as the intensity of each voxel replaced by weighted average value of the intensities of its own and neighboring voxels [59].

In the smoothing step of SPM12, the images from the normalization step are smoothed with a Gaussian filter with a size (FWHM) of 0.8mm.

3.3.1.6 Filtering

This filtering step is performed with GRETNA, which is also a toolbox about neuroscience in Matlab. The filtering step is similar to spatial filtering but the images are processed across time to reduce some temporal noise and non-neurological signals. Therefore, the smoothed images are band-pass filtered at 0.01-0.1Hz, all the signals out of the band will be removed.

3.3.2 Static correlation analysis

One of techniques used to analyze the fMRI images is static correlation analysis. From the previous study, the functional connectivity between these ROIs during a long scanning period is always regarded as constant, so one average static correlation matrix can be obtained over this long scanning time. The correlation coefficients are used in the static correlation analysis. The correlation coefficients are the measure for the degree of dependence between two variables and these are the elements in the static correlation matrix. The correlation coefficient between two variables (x and y) can be calculated using the following formula:

$$\rho_{xy} = \frac{1}{N}\sum_{n=1}^{N}\frac{(x(n)-\mu_x)(y(n)-\mu_y)}{\sigma_x\sigma_y}$$

Where N is the number of samples, μ_x and μ_y are the mean values, and σ_x and σ_y are the standard deviations of the signals.

In the static correlation matrix, each row and each column represent a region of interest (ROI), and the elements are the correlation coefficients between each connection of ROIs to indicate the functional connectivity between these ROIs. One example of static correlation matrix is shown in Figure 15. This matrix can be seen as a table containing the different values of correlation coefficients between each variable and the others.

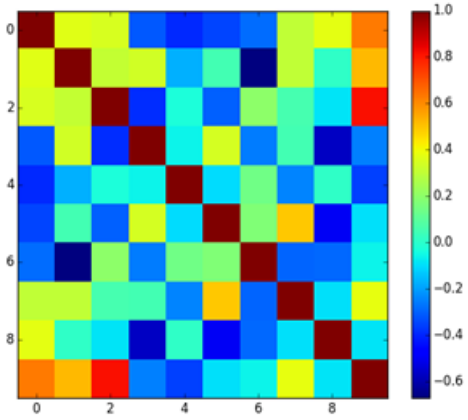

Figure 15: Example of static correlation matrix

3.3.3 Sliding window technique

Recently, the most commonly used method for examining dynamics in resting-state functional connectivity has been the sliding window technique [60]. Sliding window technique can be used to obtain correlation matrices which vary over time. In this method, a time window of fixed length is selected, and the data points within this window are used to calculate correlation matrix of different regions of interest (ROIs). The window is shifted in time by a fixed step length which defines the overlap between two windows. We can get the time-varying behavior of chosen matrix in quantity over the scanning duration.

The sliding window technique was performed on a series of preprocessed fMRI scans. Except for these fMRI images, a label mask of the rat brain is also necessary to achieve sliding window approach. The label mask was used to divide the rat brain into different regions of interests. Between two of these regions of interest, the correlation coefficient can be calculated and the correlation coefficients of all the regions of interest can form the correlation matrix.

3.3.3.1 Label mask of rat brain

After the preprocessing steps, we can obtain three time series of preprocessed fMRI images for one subject. The number of slices is set as 16, and there are 300 timepoints (600s) for one time series. The dimension of one slice is 80×80. So for each one time series (300 timepoints), the size of fMRI images can be expressed as $80 \times 80 \times 16 \times 300$. This label mask was made slice by slice by comparing with anatomical atlas to distinguish the different ROIs. And there are 38 ROIs in the rat brain fMRI image, and these are shown in the Table 1. There are two examples of label mask and corresponding same slice fMRI image which are shown in Figure 16 and Figure 17. There are no ROIs in the label mask before the 4th slice and after the 14th slices. All the slices from the 4th slice to 14th slice of label mask and

corresponding fMRI image are shown in Figure B in annexes B. I have marked and pointed out all the ROIs with the number to show the ROIs in the label mask image clearly.

Table 1: 38 ROIs of the label mask

1	Pir_r	Piriform Cortex	20	Pir_l	Piriform Cortex
2	RSC_r	Retrosplenial Cortex	21	RSC_l	Retrosplenial Cortex
3	Vis_r	Visual Cortex	22	Vis_l	Visual Cortex
4	Hip_r	Hippocampus	23	Hip_l	Hippocampus
5	Th_r	Thalamus	24	Th_l	Thalamus
6	Cg_r	Cingulate Cortex	25	Cg_l	Cingulate Cortex
7	SSC_r	Somatosensory Cortex	26	SSC_l	Somatosensory Cortex
8	MC_r	Motor Cortex	27	MC_l	Motor Cortex
9	PtA_r	Parietal Association Cortex	28	PtA_l	Parietal Association Cortex
10	PrL_r	Prelimbic Cortex	29	PrL_l	Prelimbic Cortex
11	PtP_r	Posterior Parietal Cortex	30	PtP_l	Posterior Parietal Cortex
12	CPu_r	Caudate Putamen	31	CPu_l	Caudate Putamen
13	Au_r	Auditory Cortex	32	Au_l	Auditory Cortex
14	DLO_r	Dorsolateral Orbital Cortex	33	DLO_l	Dorsolateral Orbital Cortex
15	TeA_r	Temporal Association Cortex	34	TeA_l	Temporal Association Cortex
16	GP_r	Globus Pallidus	35	GP_l	Globus Pallidus
17	Acb_r	Nucleus Accumbens	36	Acb_l	Nucleus Accumbens
18	Sep_r	Septum	37	Sep_l	Septum
19	Ins_r	Insula	38	Ins_l	Insula

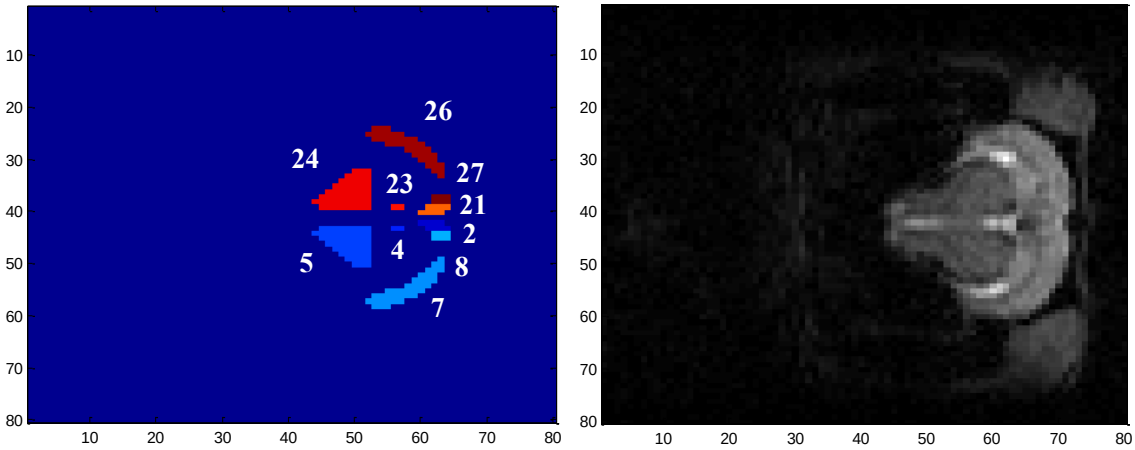

Figure 16 The 8th slice of label mask (left) and corresponding fMRI image (right)

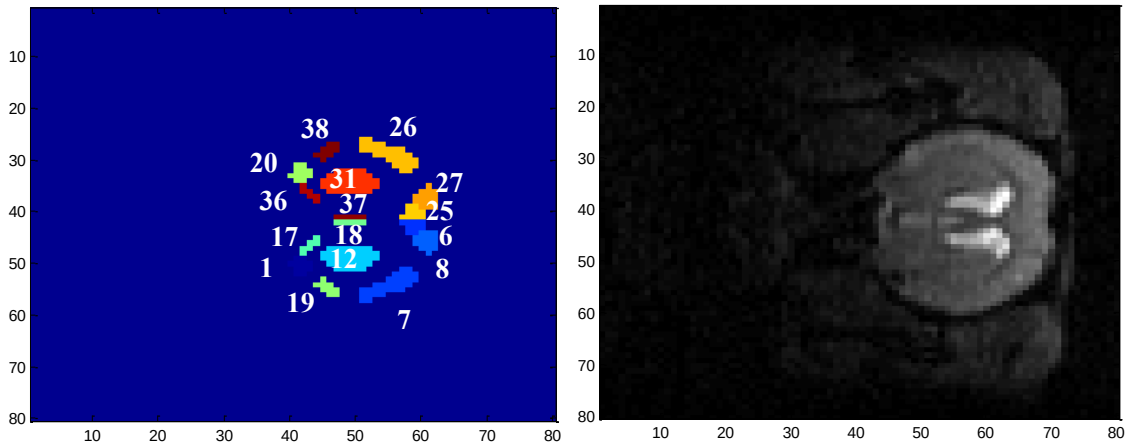

Figure 17 The 11th slice of label mask (left) and corresponding fMRI image (right)

3.3.3.2 Sliding window analysis

Using the same data, sliding window correlation was performed using window lengths of 30, 50 and 100 seconds with step length of 1TR (2s). We can find greater variance observed when shorter window lengths were used from the results.

When the window length is short, we can observe more fluctuations of correlation time courses, because there are fewer points available for computing functional connectivity, and also there will be more sensitivity to capture real fluctuations. On the other hand, when the window length is large, fewer changes will be observed. The connectivity measurement is computed over too many timepoints, it may be less able to describe fast changes. So normally, the window length should be around 30-60s, which have been able to produce robust results in conventional acquisition [60]. Therefore, the optimal window length and step length were 50 seconds and 1TR(2s) which were used in this master thesis to obtain the final results.

The whole process from label mask and fMRI data to sliding window approach was shown in Figure 18. Because of 38 ROIs in the label mask, there are 38 signals during 300 timepoints in the subject time courses. When the optimal window length and step length are selected, each two of the signals within the window are used to calculate correlation coefficient, and all the correlation coefficients of different connections of windowed signals can form one correlation matrix. After the window is shifted in time by a fixed window length, new correlation matrices can be obtained according to the same rule. Lastly, all the matrices are aggregated across subjects.

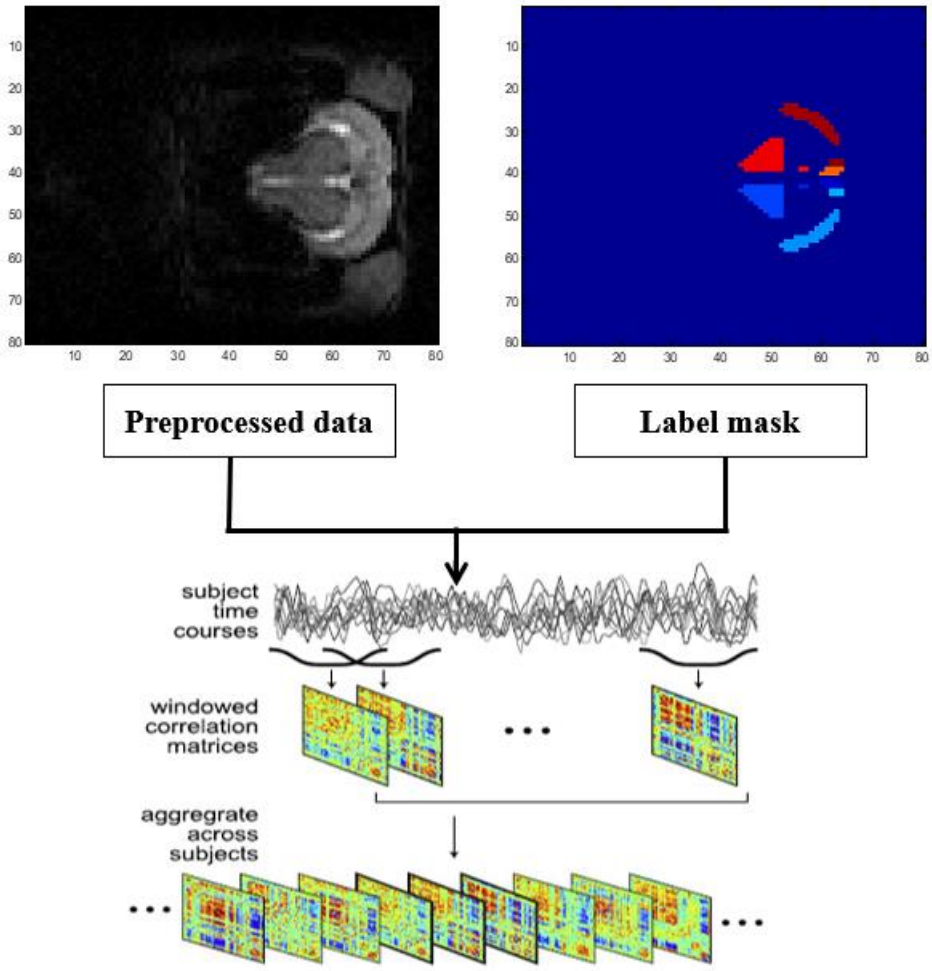

Figure 18: The overview of the analysis steps from the preprocessed data and the label mask

3.3.4 K-means clustering

When we have obtained a series of windowed correlation matrices from sliding window technique step, all the series of correlation matrices of healthy rats and epileptic rats are put together to complete clustering to keep the same clustering standard between them.

K-means clustering algorithm was used to divide these dynamic FC matrices into separate clusters to observe the recurrence of patterns of dFC connectivity within subjects across time [61]. The data can be divided into a set of clusters to maximize the correlation within a cluster to the cluster centroid. The optimal number of clusters (k value) was estimated using elbow criterion, which is defined as the ratio of within cluster to between cluster distances [61]. An optimal k of 7 was obtained using this method with the function in Matlab. There are 38 ROIs, so between each pair of ROIs, and we can obtain the FC matrix (38×38). The optimal window length is 25 timepoints (50s) and step length is 1 timepoint (2s), so the number of windows for each time course can be calculated as

$$\mathrm{WN} = \frac{(300-WL)}{SL} + 1 = 276$$

There are six healthy and six epileptic (KA) rats in this experiment, and each subject has three sessions, so $276 \times 12 \times 3 = 9936\,\text{instances}$ need to be divided. These instances can be clustered to 7 states, so each functional connectivity matrix represents the centroid of a cluster and belongs to one state.

The results of k-means clustering step show the relationship between different states and time series, so we can acquire how often each state occurs and how often there is a change of states. We can also compare the difference of these results between healthy and epileptic rats to complete the statistical analysis.

Chapter 4 Results

4.1 Introduction

For the initial fMRI data, the preprocessing steps can be completed with SPM. After the preprocessing steps of fMRI images of rat brains, the preprocessed images can be analyzed with different techniques. At first, the analysis of static functional connectivity can be performed with static correlation matrix to represent the functional connectivity between all ROIs. Then, for dynamic functional connectivity, the sliding window technique is applied with GRETNA. A series of window length and step length are used and compared to find the optimal ones. After this step, we can obtain a series of correlation matrices. The k-means clustering can divide these matrices into seven states. From the results of this step, we can find the number of occurrences of different states in healthy and epileptic rats and also investigate the difference of the number of transitions between them.

4.2 Static functional connectivity analysis

Although the functional connectivity between each pair of ROIs varies over time in reality, we can obtain one average correlation matrix over time series for each rat, and the mean and standard deviation (SD) of all correlation coefficients in this matrix are shown in Table 2. And then, we can acquire the average correlation matrix for all healthy and epileptic rats separately. The average correlation matrix over time for all epileptic rats is shown in Figure 19, and the average correlation matrix over whole time series for all healthy rats is shown in Figure 20.

From the comparison of the values in the table, we can find that the mean of correlation coefficient for all healthy rats is higher than epileptic rat, while the standard deviation of all healthy rats is lower than epileptic rats. From these two figures of average correlation matrix, we can also find visually the values of correlation coefficients between most of connections of ROIs for healthy rats are higher than epileptic rats. In order to show the difference between these two average correlation matrices clearly, we can obtain the subtraction of these two matrices by average correlation matrix for healthy rats subtracting the matrix for epileptic rats. The result of subtraction is shown in one same dimension matrix, which is shown in Figure 21. In addition, we have applied statistical analysis method, which is Mann-Whitney U test, on the data of these two matrices to find if there is a significant difference between these two matrices. Corresponding Matlab function is used to calculate the p value and we can find the p value is much smaller than 0.05, and it indicates there is a significant difference of the values in these two matrices, and we can further obtain that there is a large difference of functional connectivity between the 38 ROIs in the brains for healthy and epileptic rats.

Table 2: Mean and SD of correlation coefficient for each rat

Epileptic rats	Mean and SD	Healthy rats	Mean and SD
1	0.4782 ± 0.0063	1	0.7299 ± 0.0095
2	0.6432 ± 0.0069	2	0.7697 ± 0.0062
3	0.5059 ± 0.0248	3	0.7576 ± 0.0052
4	0.5456 ± 0.0194	4	0.6276 ± 0.0059
5	0.5565 ± 0.0052	5	0.6675 ± 0.0079
6	0.7851 ± 0.0060	6	0.7866 ± 0.0036
Mean and SD (all epileptic rats)	0.5858 ± 0.0062	Mean and SD (all healthy rats)	0.7232 ± 0.0037

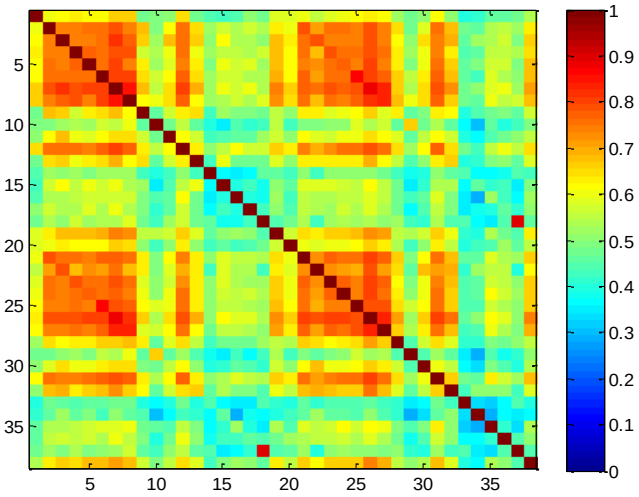

Figure 19: Average correlation matrix over time for all epileptic rats

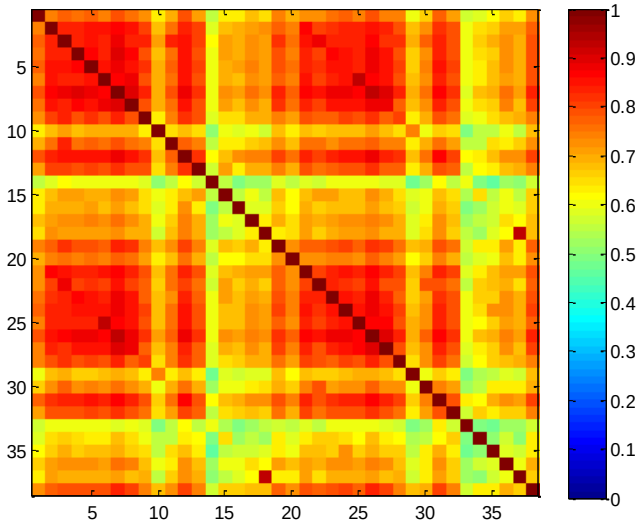

Figure 20: Average correlation matrix over time for all healthy rats

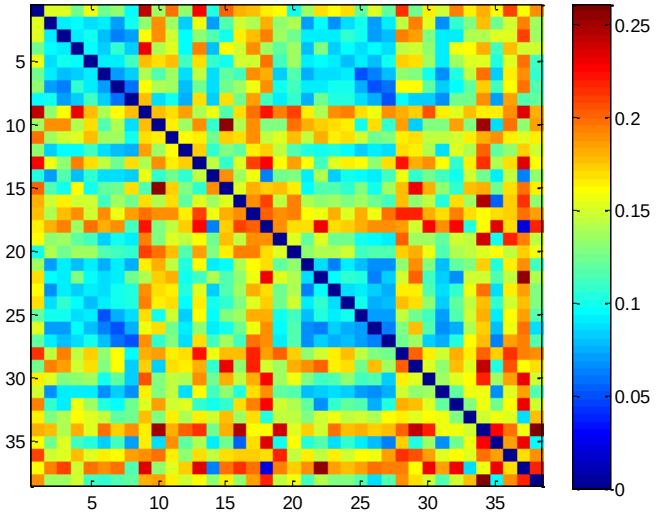

Figure 21: Subtraction of two matrices for healthy and epileptic rats

4.3 Dynamic functional connectivity analysis

From the recent research, we can find that the functional connectivity between connections of ROIs in rat brains are dynamic, so the correlation coefficient between two ROIs changes over time (window number). In our study, one example connection of ROIs which are left hippocampus (Hip_l) and left thalamus (Th_l) is chosen to investigate the time-varying correlation coefficient. The location of Hip_l and Th_l in correlation matrix can be found from Table 1, which is shown in Figure 22Figure 22. When window length (WL=25 timepoints=50s) and step length (SL=1 timepoint=2s) are selected, the window number WN is 276, which can be calculated from the same formula above. And then, we can obtain the relationship between correlation coefficient (between Hip_l and Th_l of one healthy rat brain) and window number (time), which is shown in Figure 23. This graph clearly shows that the correlation coefficient is not unchanged or static and it is varying over time, which can indicate the fact of dynamic functional connectivity.

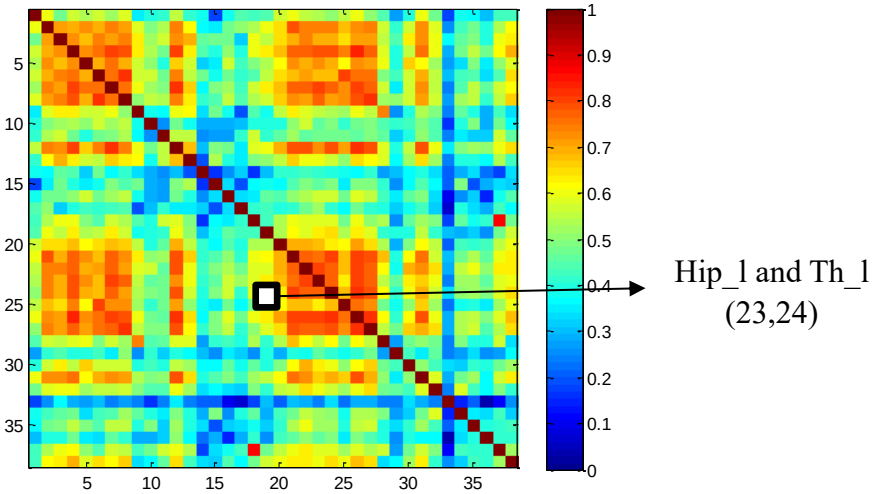

Figure 22: The location of the pair of ROIs (Hip_l and Th_l) in correlation matrix

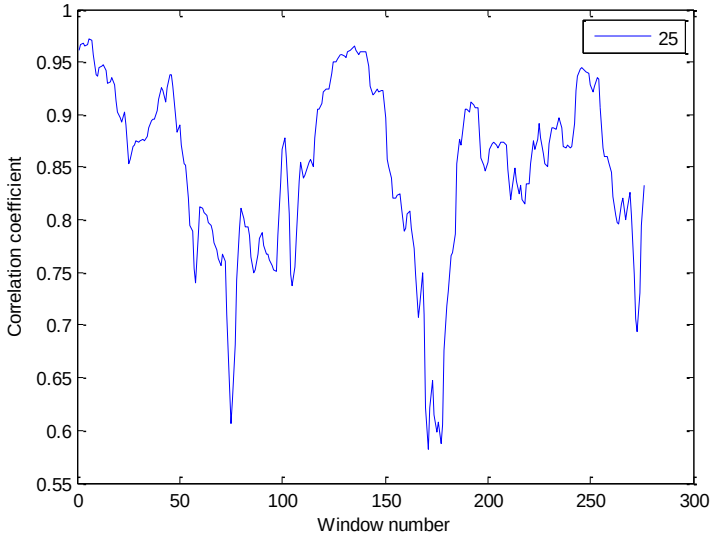

Figure 23: Correlation coefficient between two ROIs varies over window number

4.4 Sliding window technique

To complete the analysis of dynamic functional connectivity over one time series (300 timepoints), sliding window technique is applied to obtain a series of correlation matrices. But before that, we need to find the optimal window length and step length.

4.4.1 Optimal window length and step length

Sliding window correlation was plotted as a function of time for each scan using window lengths of 30, 50 and 100 seconds with step length of 2s. One example from the first scan of the first healthy rats is shown in Figure 24. We can find that all correlation time courses exhibited variance over time. Comparing the difference between correlation time courses of different window length, we can observe greater variance when shorter window lengths are used. These results are consistent with previous findings in another research [60]. Based on this finding, the window length should be neither too short nor too large, and it should be around 30-60s. For step length, 1TR (2s) is chosen in this study. Therefore, the optimal window length and step length which are chosen in this study are 25 timepoints (50s) and 1 timepoint (2s) separately.

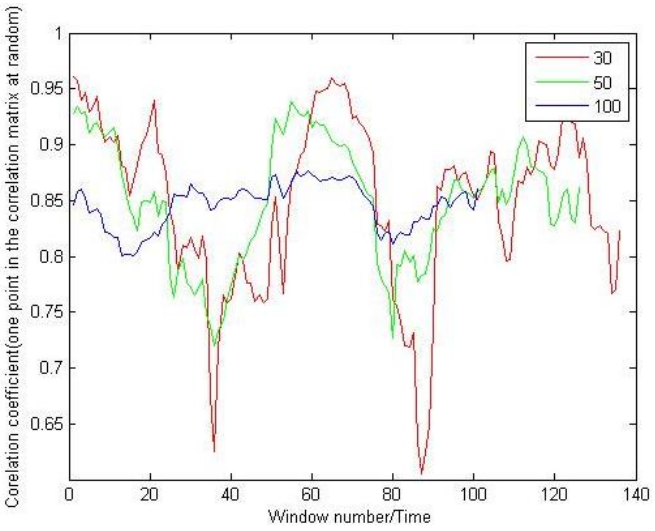

Figure 24: Correlation is plotted as a function of window number for different window lengths [s]

4.4.2 Sliding window technique

Sliding window technique was performed with GRETNA in this study, and one example protocol of this software to complete sliding window technique was shown in Figure 25. The window number for each scan per rat (WN) is 276, which can be calculated by the same formula above. After this step, we can obtain a series of correlation matrices for each scan per rat.

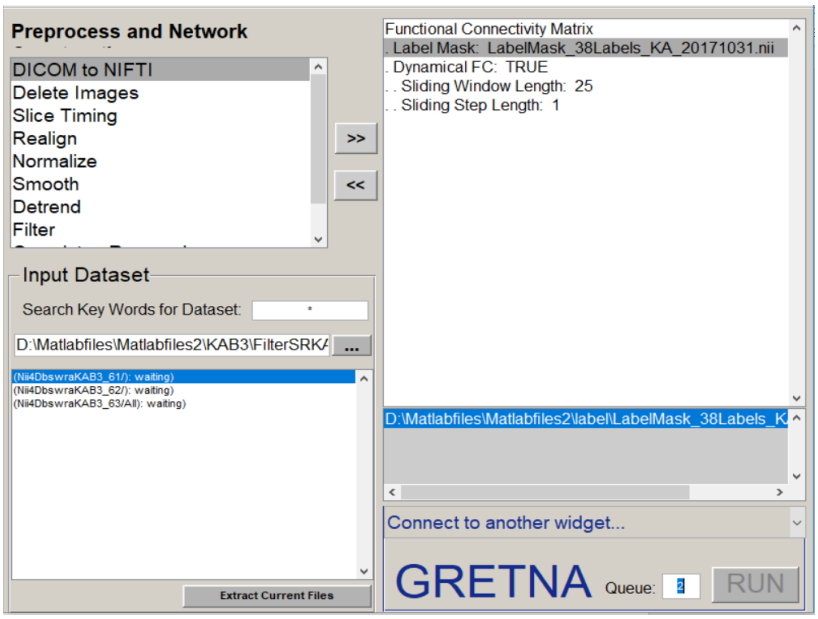

Figure 25: Protocol of GRETNA to complete sliding window technique

4.5 Clustering

K-means clustering is used to cluster all the dynamic FC matrices for all scans including epileptic and healthy rats. An optimal k of 7 is found using elbow criterion with Matlab. From the materials and methods part of this thesis, we can know that there are six healthy and six epileptic rats in this experiment and each subject is scanned three times. The window number each scan per subject is 276, so there are $276 \times 6 \times 2 \times 3 = 9936$ instances in total to divide into separate clusters. The results of k-means clustering show that there are seven states for all dFC matrices, and the cluster centroids for FC states 1-7 are shown in Figure 26.

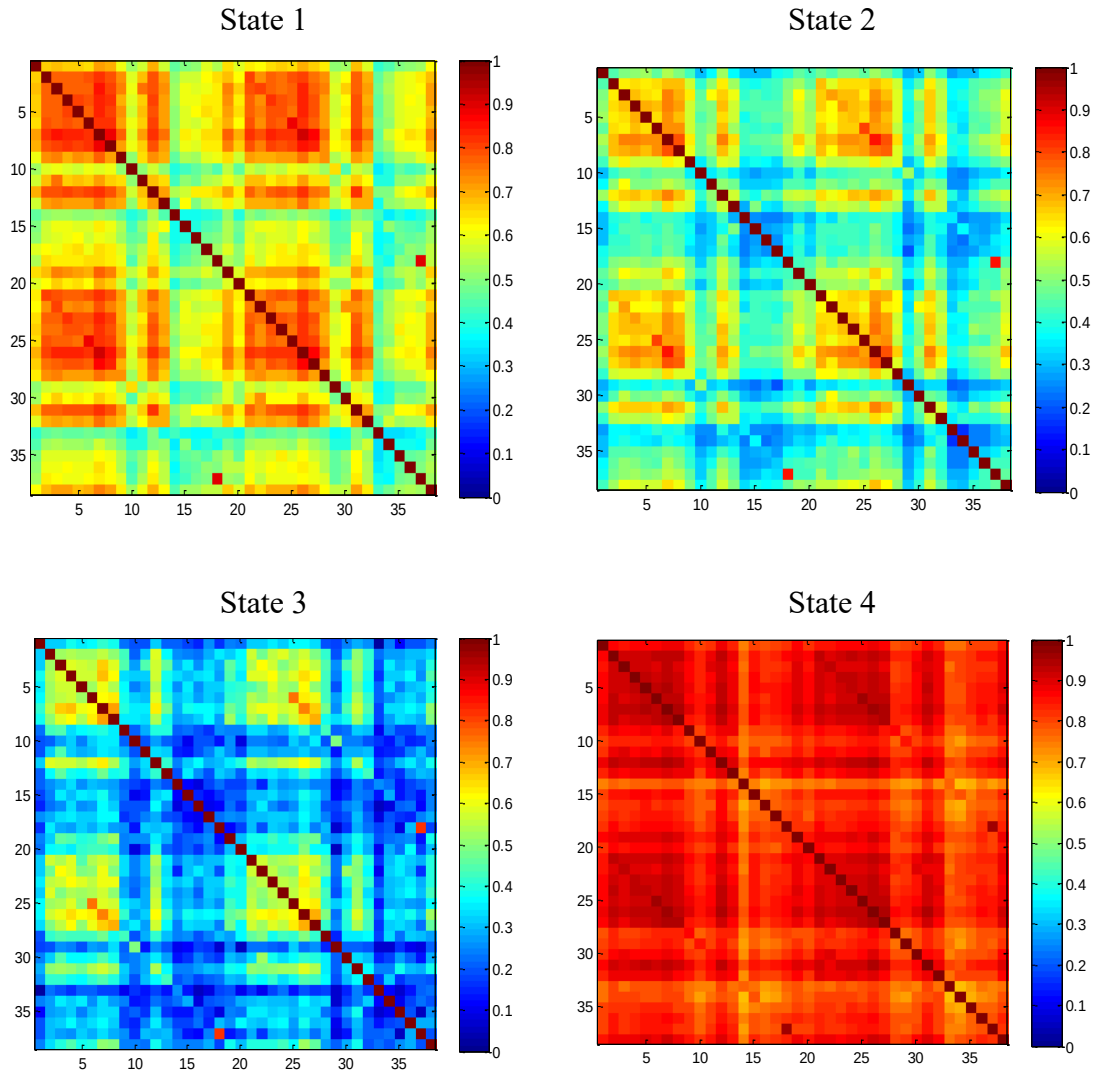

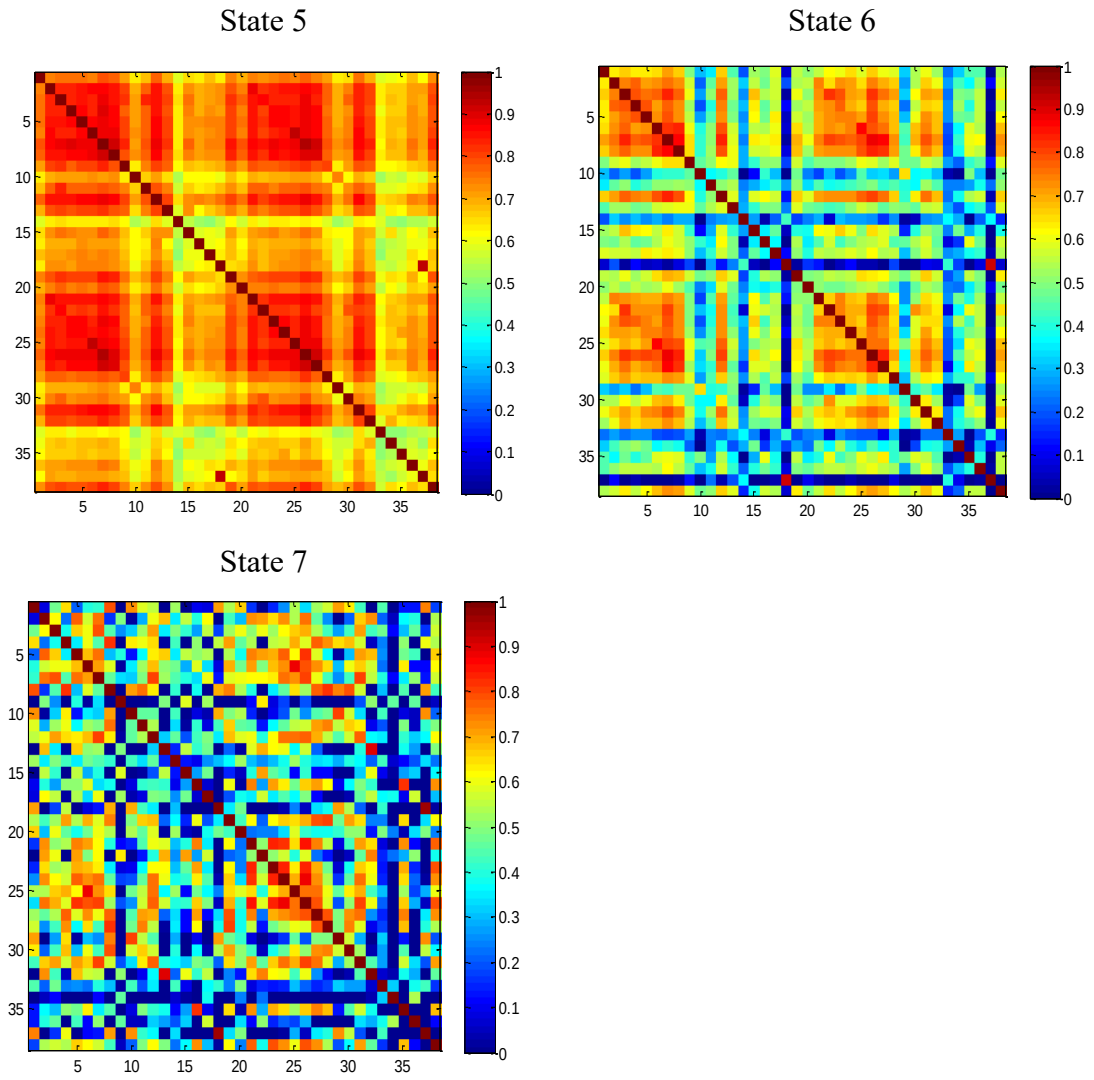

Figure 26: Correlation matrices of cluster centroids for FC States 1-7

We can clearly observe that there are huge differences of the values of correlation coefficients in these correlation matrices of seven states. The values of correlation coefficients in State 1, State 4 and State 5 are much higher than other States generally, and larger value in the correlation matrix indicates stronger functional connectivity. The highest and lowest values, the mean and standard deviation in each state are shown in the Table 3.

Table 3: Statistical results of the values in correlation matrices of seven states

States	Maximum	Minimum	Mean±SD	Rank
State 1	0.914	0.329	0.6271 ± 0.0042	3
State 2	0.859	0.162	0.4947 ± 0.0047	4
State 3	0.82	0.0308	0.3497 ± 0.0094	7
State 4	0.964	0.676	0.8460 ± 0.0021	1
State 5	0.939	0.508	0.7309 ± 0.0031	2
State 6	0.912	0.018	0.4846 ± 0.0324	5
State 7	0.964	0.03	0.3726 ± 0.0606	6

Table 4: General top ten connections of ROIs for all states

Rank	1	2	3	4	5	6	7	8	9	10
ROIs	SSC_l, SSC_r	Sep_l, Sep_r	Cg_l, Cg_r	MC_r, SSC_r	MC_l, SSC_r	MC_l, MC_r	MC_l, SSC_l	SSC_r, Hip_r	SSC_r, Hip_r	SSC_l, Hip_r

From the Table 3, we can find that the mean values of correlation matrix in State 1, State 4, State 5 are above 0.5, which means general stronger functional connectivity of all ROIs in these states. However, the mean values of correlation matrix in State 2, State 3, State 6 and State 7 are lower than 0.5, which means weaker functional connectivity of the ROIs in these states.

To investigate detailed connections of ROIs which show stronger functional connectivity, we have obtained the top ten connections of ROIs for all seven states, which are shown in Table A in annexes. From this table, we can find many top ten connections of ROIs are the same in all states, so the list of general top ten connections of ROIs for seven states is shown in Table 4. From these connections, the two strongest correlations occur between left and right somatosensory cortex (SSC_l and SSC_r), and left septum and right septum (Sep_l and Sep_r) while left dorsolateral orbital cortex and temporal association cortex (DLO_l and TeA_l) exhibit a weaker correlation.

4.5.1 Number and percentage of occurrences of different states

When k-means clustering is completed to obtain seven states, the statistical calculation of the clustering results can be done. From the description above, we can know that 9936 instances in total need to be divided into seven states. Therefore, the number of occurrences of each state is the number of instances (matrices) which are divided into this state in healthy or epileptic rats. The percentage of occurrences of different states is the number of occurrences of each state divided by the total number of instances in healthy and epileptic rats.

We also want to investigate how stable the clustering or pattern between six healthy and epileptic animals is. To quantify this, the coefficient of variation (CV) needs to be calculated. The coefficient of variation (CV) is defined as the ratio of standard deviation σ to the mean μ, which is shown in this formula:

$$\mathrm{CV} = \frac{\sigma}{\mu}$$

CV shows the extent of variability in ration to the mean of the population. CV is also a measure for reproducibility of the data. This coefficient can remove the effect of different mean on the degree of variation.

The percentage and the numbers of occurrences of different states for healthy rats are shown in Table 5. The coefficient of variation for each state or pattern can also be calculated by the formula above, which is also shown in Table 5. The percentage and numbers of occurrences of different states for epileptic rats, and the corresponding CV for each state or pattern are shown in Table 6. One graph to compare the number of occurrences of different states is shown in Figure 27.

Table 5: Percentage and the number of occurrences of different stats for healthy rats

States	Healthy rats						Sum	CV (SD/Mean)	Rank	Percentage
	1	2	3	4	5	6				
State1	191	266	111	366	306	158	1398	0.413	2	28%
State2	21	47	17	229	152	68	534	0.948	4	11%
State3	0	5	1	34	44	32	116	1.008	5	2%
State4	166	237	289	35	84	268	1079	0.574	3	22%
State5	415	273	404	158	218	302	1770	0.344	1	36%
State6	35	0	6	6	24	0	71	1.215	6	1%
State7	0	0	0	0	0	0	0	0	7	0
Sum	4968									100%

Table 6: Percentage and the number of occurrences of different stats for epileptic rats

States	Epileptic rats						Sum	CV (SD/Mean)	Rank	Percentage
	1	2	3	4	5	6				
State1	85	352	119	146	260	110	1072	0.586	2	22%
State2	414	111	113	196	359	26	1219	0.752	1	24%
State3	295	91	119	40	113	3	661	0.917	4	13%
State4	0	48	0	7	0	383	438	2.096	6	9%
State5	1	224	20	163	67	302	777	0.928	3	16%
State6	33	2	457	0	29	4	525	2.075	5	11%
State7	0	0	0	276	0	0	276	2.449	7	5%
Sum	4968									100%

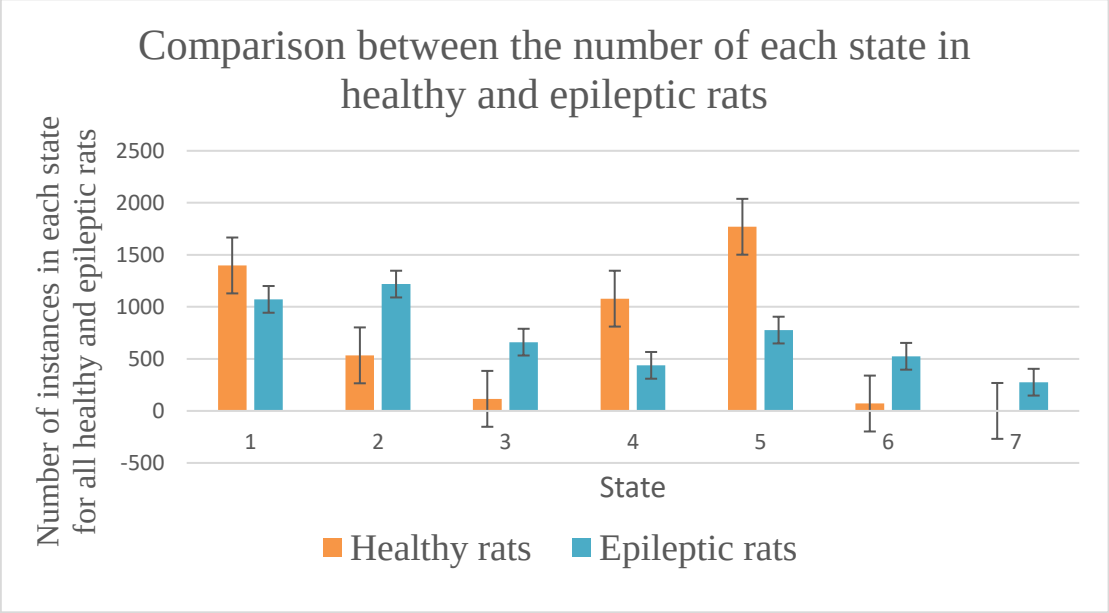

Figure 27: Comparison between the number of occurrences of each state in healthy and epileptic rats

From the graph and table above, we can find that there is a big difference between healthy and epileptic rats in most of states. The number and percentage of occurrences of State 1, State 4 and State 5 for healthy rats are higher than epileptic rats and the number and percentage of occurrences of State 2, State 3, State 6 and State 7 for epileptic rats are higher than healthy rats.

For the coefficient of variation, we can compare the values of CV for each state or pattern. Higher CV shows high variability and low stability between all healthy or epileptic rats. Distribution with $CV < 1$ is considered low-variance, while those with $CV > 1$ are considered high-variance [62]. For healthy rats, CV of State 1, State 4 and State 5 are much lower than other states, so this indicates the patterns of State 1, State 4 and State 5 are more stable than other patterns. Only few healthy animals have the patterns of State 3 and State 6, and no healthy animals have the pattern of State 7, so this indicates low stability and reproducibility of these patterns for healthy rats. For epileptic rats, the patterns of State 1, State 2 and State 3are more stable than others. And we can also notice that few epileptic rats have State 4 and State 5, and only one epileptic rat has the pattern of State 7, which indicates low stability and low reproducibility of these patterns for epileptic rats.

In addition, we have to apply statistical analysis approach on these data to find if there is a significant difference between these two kinds of rats. Statistical analysis is a necessary tool to prove the findings of results and bring some reasonable support to investigate if there is a significant difference between two groups of experiments. In this study, Mann-Whitney U test [63] is used to test whether the difference between healthy and epileptic rat groups is significant.

Mann-Whitney U test is a nonparametric test of null hypothesis which it is equally likely that a randomly selected value from one sample will be greater or less than another randomly selected value from a second sample.

The statistical analysis is applied to prove the significant difference between the number of occurrences of each state for epileptic and healthy rats. To complete the Mann-Whitney U test, the corresponding Matlab function is used. And for each state, the p value is calculated of the number of epileptic and healthy rats, and all the p values of different states are shown in Table 7. The null hypothesis of this test is there is no difference between epileptic and healthy rats in the number of occurrences of different states, and the significance level is $\alpha = 0.05$. Therefore, there is a significant difference ($p<0.05$) of the number of occurrences of State 3 between the epileptic and healthy rats. However, if the $p<0.1$, there is a trend towards significance or it is marginally significant, and it can indicate there is a marginally significant difference of the number of occurrences of that state between healthy and epileptic rats, such as the State 4 and State 5. If the p value is higher than 0.1, there is no significant difference between healthy and epileptic rats, such as state 1, state 2, state 6 and state 7.

Table 7: P value of different states

	State 1	State 2	State 3	State 4	State 5	State 6	State 7
P value	0.2403	0.1797	0.0411	0.0909	0.0714	0.6667	1

There is a significant difference of the number of occurrences of State 3 between epileptic and healthy rats, and the number and percentage of occurrences of State 3 for epileptic rats are much higher than healthy rats. From Table 3, the mean of correlation matrix in State 3 is much lower than other states, which indicates the weaker functional connectivity in State 3 than others. Therefore, the state of weaker functional connectivity (State 3) occurs more in epileptic rats.

4.5.2 Number of transitions of states for each rat

Except for the number of different states, another important result which we can obtain from the k-means clustering is the number of transitions of states for each rat. The transitions of states indicate the frequency of the change of state. One example to show the transitions of states of healthy rats for one scan is shown in Figure 28. After the statistical calculation, the number of transitions for each scan per rat are shown in Table 8.

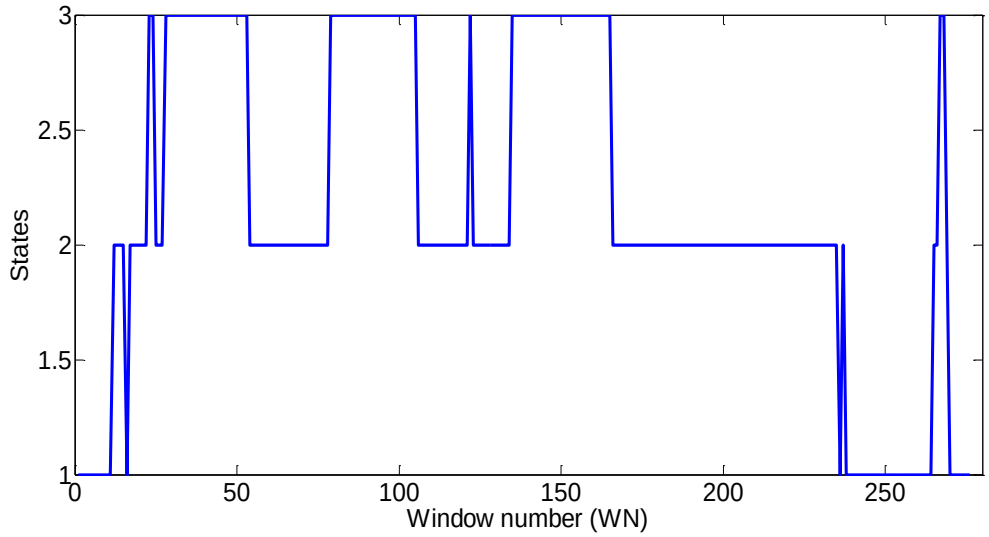

Figure 28: The relationship between states and the window number for one scan

Table 8: The number of transitions for each scan per rat

Rats	Scans	Healthy	Sum	Epileptic	Sum
1	1	38	99	21	56
	2	27		14	
	3	34		21	
2	1	19	70	26	89
	2	27		22	
	3	24		41	
3	1	30	82	28	54
	2	23		8	
	3	29		18	
4	1	37	94	31	58
	2	26		1	
	3	31		26	
5	1	41	103	30	91
	2	28		27	
	3	34		34	
6	1	29	68	8	62
	2	16		28	
	3	23		26	

From the results of the table above, the mean and standard deviation of the number of transitions for healthy and epileptic rats can be calculated. The coefficient of variation (CV) of healthy and epileptic rats can also be obtained from the mean and standard deviation. The mean and standard deviation for healthy rats is 28.67 ± 6.53, and CV is 0.228. The mean and standard deviation for epileptic rats is 22.78 ± 10, and CV is 0.439.

From the values of mean and standard deviation above, we can find that the average number of transitions in healthy rats is higher than epileptic rats. The standard deviation of all healthy rats is lower than epileptic rats, and also CV for healthy rats is lower than epileptic rats, which means the data about the number of transitions of healthy rats is more stable than epileptic rats. And there would be a large difference between the number of transitions for different epileptic rats.

For the statistical analysis, the Mann-Whitney U test can also be applied on the sum number of transitions of states for each rat. Therefore, there are six values of number of transitions for each group and we want to compare these by this statistical test. This test is used to investigate if there is a significant difference of number of transitions between six healthy and epileptic rats. The p value which is calculated with this statistical test is 0.0649 ($0.05 < p < 0.1$), so we can't reject the null hypothesis without increasing the significance level, we can also find there is a marginally significant difference of the number of transitions of states between six healthy and epileptic rats, and the number of transitions of states in healthy rats is higher than epileptic rats.

Chapter 5 Discussion

In this study, we have explored the dynamic functional connectivity in the rat model of TLE and found the difference between healthy and epileptic rats in the percentage and number of states and the number of transitions of states with sliding window technique and clustering.

5.1 Functional connectivity in temporal lobe epileptic rats

5.1.1 Static functional connectivity analysis

In our study, for sFC analysis results, two average correlation matrices of healthy and epileptic rats have been obtained. We can find that the mean value of correlation coefficients between these ROIs for healthy rats is higher than in epileptic rats, which can indicate that healthy rat brains have stronger functional connectivity between these ROIs than epileptic rat brains.

One current study has compared the mean correlation matrix across all the subjects within the healthy and epileptic group (Luo C et al., 2011). And it reveals that functional connectivity in the epilepsy patient group appeared to be less than healthy group [64]. In this study, to compare connectivity of each pair regions, the correlation of one third of pairs of regions were decreased significantly ($p < 0.05$) in the patient group, and no significant increase of correlation of the pair of regions was observed in the patient [64]. Moreover, they have found the decreased functional connectivity in epilepsy patient may be related to attention and memory loss, just like the cases in Alzheimer's disease and schizophrenia [64].

Other previous studies (Henkin et al., 2005) have found that cognitive and behavioral deficits are exhibited in epilepsy patients, such as attention, memory, and language function [65]. In addition, reduced connectivity strength within the temporal lobe was reported in resting-state fMRI studies in TLE patients (Bettus et al., 2009) [66].

The findings from these studies about epilepsy patients are consistent with our findings to support our study.

5.1.2 Dynamic functional connectivity analysis

The dynamic functional connectivity in the rat model of TLE has been explored and indicated in this thesis. For dFC analysis results, seven states for all dFC matrices have been obtained. The mean values of the correlation matrices of these states have been calculated and compared, and the matrix of State 3 has the lowest mean value of correlation coefficients compared to other states, which is shown in Figure 29. The matrices of State 4 and 5 have the highest mean value of correlation coefficients compared to others, which are shown in Figure 30.

In addition, top ten connections of these ROIs for all states have been found. As expected, the strongest correlations occur between homologous areas in the left and right cortex (Keilholz S D et al.,2013) [48]. Left and right somatosensory cortex (SSC_l and SSC_r), and left septum and right septum (Sep_l and Sep_r) show stronger correlation than others, while left dorsolateral orbital cortex and temporal association cortex (DLO_l and TeA_l) exhibit a weaker correlation than others. Although both of SSC_l and SSC_r, and Sep_l and Sep_r are mirrored pairs, Sep_l and Sep_r are closely located to each other from the anatomy of brain. Therefore, left and right somatosensory cortex exhibit highest correlation, and this high correlation pair is more meaningful than Sep_l and Sep_r, which is similar to this seen in previous work (Williams K A et al.,2010) [67].

From the further investigation of the number and percentage of the occurrences of different states, we have found there is a significant difference of the percentage and number of occurrences of State 3 between epileptic and healthy rats, and the number and percentage of occurrences of State 3 for epileptic rats are much higher than healthy rats. Therefore, we can further infer that more dFC matrices of epileptic rats are divided into State 3 than healthy rats, and the majority of epileptic rat brains have the same characteristic as the FC of State 3. This can indicate that epileptic rat brains have weaker functional connectivity than healthy rats. In addition, the number and percentage of occurrences of State 4 and State 5 for healthy rats are higher than epileptic rats, so these two states with the highest correlation coefficients occur marginally significantly more in healthy rats than in epileptic rats.

State 3

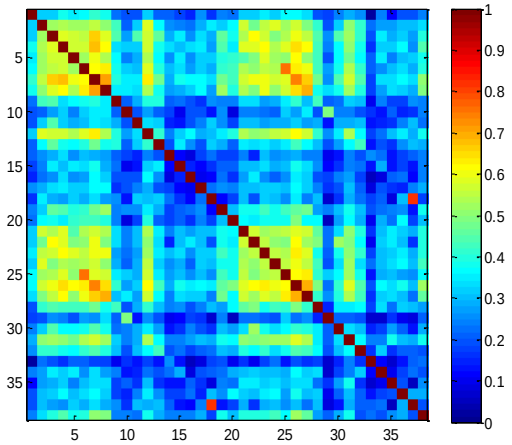

Figure 29: The correlation matrix of State 3

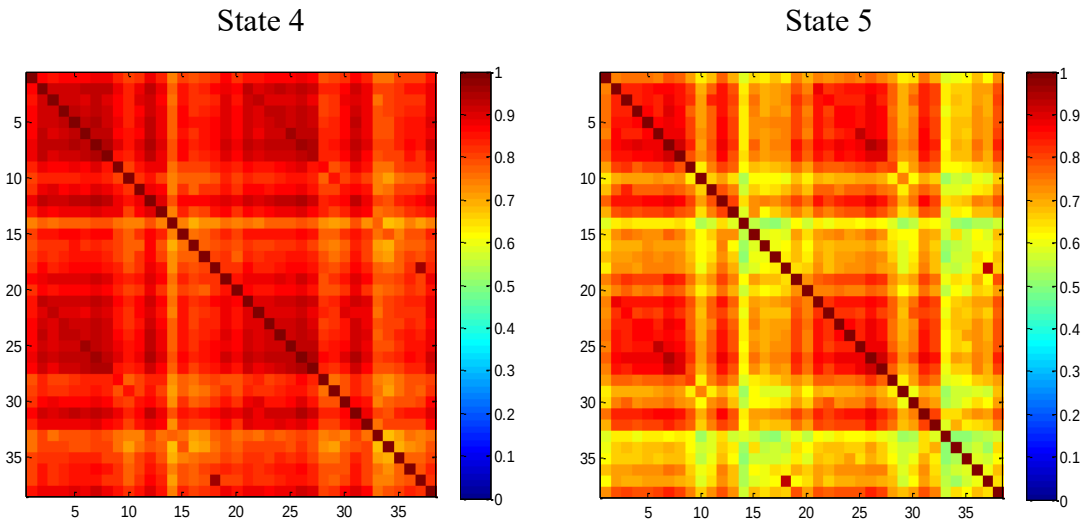

Figure 30: The correlation matrices of State 4 (left) and State 5 (right)

Another one study about dynamic functional connectivity in generalized tonic-clonic seizure patients have found that patients had significantly shorter dwell time in State 4 (high correlation state), and dwell time is measured as the average number of windows in the same state (Liu F et al. 2017) [68]. In addition, the fraction of time spent in this high correlation state was shorter than healthy controls, and fraction of time spent in each state is measured as the proportion of the windows in each state [68].

From one study about focal epilepsy rat model, interhemispheric functional connectivity was reduced in the epileptic group, while interhemispheric functional connectivity remained stable over time in the control animals (Willem M.Otte et al. 2012) [69]. Increased intrahemispheric functional connectivity was found in both hemispheres in epilepsy rats [69]. Focal epilepsy resulted in significant lower fractional anisotropy (FA) values in white matter [69].

These findings about dwell time in dFC analysis and focal epilepsy rat model are consistent with our findings to support our results.

5.1.3 Number of transitions

From the results of this study about transitions of states, we have found there is a marginally significant difference of the number of transitions of states between healthy and epileptic rats. The mean and standard deviation for healthy rats is 28.67 ± 6.53, and the mean and standard deviation for epileptic rats is 22.78 ± 10. We can find that the average number of transitions in healthy rats is higher than epileptic rats, which could indicate that the healthy rat brains are more active than epileptic rats generally. The coefficient of variation and standard deviation of all healthy rats are lower than epileptic rats, which means the number of

transitions of healthy rats is more stable and less changeable than epileptic rats.

For the transitions of functional connectivity, one study found there was a significant difference in the number of transitions between generalized tonic-clonic seizure patients and healthy controls (Liu F et al. 2017), and total number of state transitions in patients was less than that of controls, but mean transition probability was unchanged [68].

5.2 Optimal window length and step length

The choice of window size is an issue concerning the sliding window analysis. The window length should be short enough to permit the detection of fluctuations and long enough to allow estimation of FC [68]. In previous studies, the minimum window length should be larger than $1/f_{min}$,where $f_{min}$was the minimum frequency of correlation time courses [70]. In this study, a bandpass filter (0.01-0.1Hz) was applied to remove the physiological noise, so the optimal window length should be greater than (1/0.01=100s) [68]. In this study, although a series of window lengths and step length are used to make the plot of correlation coefficient as the function of time, this is not enough to find the best window length. Therefore, the optimal window length of 50s and step length of 2s are chosen empirically based on the graph which obtained from the results and previous research [71]. This previous research reported that cognitive states may be identified correctly from the covariance matrices estimated on as little as 30-60s of data. If the window size shrinks, the SNR of the estimated FC decreases because there are fewer points available for computing the functional connectivity [60].

There are some alternatives to a fixed window size, one may estimate the change points in FC to demarcate the windows [72], or use multi-scale window lengths approaches [60].

5.3 Limitations and future directions

It is still not clear whether the observed connectivity patterns are of neural origin, or whether they are patterns induced by non-neural sources. Therefore, one limitation is the observed dynamics of FC may be driven by time-varying noise (e.g. motions of subjects and psychological noises). Dynamic analysis is very sensitive to the noise, and the variations of the noise signal level across the scan which generate strong correlated signal fluctuations, can be wrongly seen as dynamic of functional connectivity. This noise may not be completely eliminated even with most powerful preprocessing techniques. Another limitation is the white noise, which can exhibit the fluctuations in common FC matrices which are observed in actual fMRI data. Therefore, the sliding window technique should be accompanied by hypothesis which are supported with appropriate statistical testing [60]. And we need to find the whether there is a significant difference of the range of sliding window variability between two ROIs between two subject populations.

Though k-means clustering is an efficient and robust partitioning algorithm, it has some limitations. It is very difficult to separate the different clusters of different sizes and densities of correlation matrices. There are some other clustering models, for example fuzzy-clustering method, which are not subject to the same limitations and may be better for FC clustering [51]. Many other approaches to identify FC states are also possible rather than clustering, such as using topological description of brain connectivity as characteristics instead of the connectivity values themselves [73]. Some models can be made to detect the change points in connectivity instead of clustering [74].

Future work will consider and develop methods for the identification of FC states and state transition. In this study, the differences between groups have been found, but the neurological meaning behind these alternations is not clear and this should be investigated in the future studies. Future work should also consider multi-modal approaches such as EEG-fMRI, to determine the electrophysiological difference between FC states [51], and also to find the mapping of cognitive states from connectivity data. Multimodal studies will also be important in determining which properties are neutrally or meaningful. Also, some techniques can be adopted from other fields for example pattern recognition from computer science. Finally, it is of importance to move from investigating the variations in FC with simple descriptive measure (for example correlation) to more complex and biologically informed models which allow serious inference of non-stationary functional network activity from fMRI data.

Chapter 6 Conclusion

In this study, the dynamic functional connectivity (dFC) is investigated using resting state fMRI (rs-fMRI) in a rat model of temporal lobe epilepsy. For static functional connectivity analysis, the average correlation matrix over time series for all healthy and epileptic rats can be obtained. From the comparison between these average correlation matrices, we can find visually the general values of correlation coefficients between ROIs for healthy rats are much higher than epileptic rats, and it can further indicate that the functional connectivity of ROIs in healthy rat brains is stronger than epileptic rats. Therefore, static analysis approaches will persist and continue to provide valuable information concerning healthy and epileptic brains of rats. However, if we desire to find a more comprehensive understanding of large-scale network activity, dynamic functional connectivity must be considered and evaluated.

For the dynamic functional connectivity, we have obtained that correlation coefficient between two ROIs (Hip_l and Th_l) changes over time (window number), and this can indicate the fact of dynamic functional connectivity at first. And then, the sliding window technique and k-means clustering have been performed. After the k-means clustering step, seven states for all dFC matrices have been obtained. From the comparison between these seven correlation matrices, we can obtain that the average values of correlation coefficients in State 1, State 4 and State 5 are higher than other states. Left and right somatosensory cortex shows the strongest correlation and dorsolateral orbital cortex and temporal cortex exhibits the weakest correlation in these high values states. In addition to the values of correlation matrices, the number and percentage of occurrences of different states and the number of transitions of states for each rat need to be investigated. Based on the statistical analysis, we have found there is a significant difference of the number of occurrences of State 3 between healthy and epileptic rats, and the number and percentage of occurrences of State 3 for epileptic rats are much higher than healthy rats. Because the mean value of correlation matrix of State 3 is much lower than other states, we can infer that epileptic rat brains have weaker functional connectivity of these ROIs than healthy rat brains. For the number of transitions of states in healthy and epileptic rats, according to the Mann-Whitney statistical analysis, we can find there is a marginally significant difference of the number of transitions of states between healthy and epileptic rats, which is the mean number of transitions in healthy rats is higher than epileptic rats, while the standard deviation of number of transitions in healthy rats is much lower than epileptic rats. Therefore, healthy rats have more transitions of functional connectivity than epileptic rats.

The dynamic functional connectivity patterns of TLE rat models have been investigated and found in this study. Future research is recommended to investigate dFC with more complex and informed model rather than correlation using new multi-modal approaches and some techniques from other fields.

References

[1] Hellier J L, Patrylo P R, Buckmaster P S, et al., "Recurrent spontaneous motor seizures after repeated low-dose systemic treatment with kainate: assessment of a rat model of temporal lobe epilepsy," *Epilepsy Research 31,* pp. 73-84, 1998.

[2] Stefaan Vandenberghe, Vincent Keereman, and Pieter van Mierlo, Neuromodulation and imaging, 2014.

[3] Bromfield EB, Cavazos JE and Sirven JI, "Basic Mechanisms Underlying Seizures and Epilepsy," in *An introduction to Epilepsy*, 2006.

[4] Jefferys, John GR, "Advances in understanding basic mechanisms of epilepsy and seizures," *Seizure-European Journal of Epilepsy,* pp. 638-646, 2010.

[5] Ogunniyi A, Osuntokun B O, Bademosi O, et al., "Risk factors for epilepsy: case-control study in Nigerians," *Epilepsia,* pp. 280-285, 1987.

[6] Fisher R S, Boas W E, Blume W, et al., "Epileptic seizures and epilepsy: definitions proposed by the International League Against Epilepsy (ILAE) and the International Bureau for Epilepsy (IBE)," *Epilepsia,* pp. 470-472, 2005.

[7] Behr C, Goltzene M A, Kosmalski G, et al., "Epidemiology of epilepsy," *Revue neurologique,* pp. 27-36, 2016.

[8] Senanayake N, Román G C., "Epidemiology of epilepsy in developing countries," *Bulletin of the World Health Organization,* p. 247, 1993.

[9] Zhao F, Kang H, You Li, Rastogi P, Venkatesh D, Chandra M., "Neuropsychological deficits in temporal lobe epilepsy: A comprehensive review.," *Annals of Indian Academy of Neurology,* pp. 374-382, 2014.

[10] Shin HW, Jewells V, Hadar E, Fisher T, Hinn A, "Review of Epilepsy-Etiology, Diagnostic Evaluation and Treatment," *International Journal of Neurorehabilitation,* 2014.

[11] Benbadis S., "The differential diagnosis of epilepsy: a critical review," *Epilepsy & Behavior,* pp. 15-21, 2009.

[12] Ho S S, Berkovic S F, Berlangieri S U, et al., "Comparison of ictal SPECT and interictal PET in the presurgical evaluation of temporal lobe epilepsy," *Annals of neurology,* pp. 738-745, 1995.

[13] Gilliam F, Wyllie E., "Diagnostic testing of seizure disorders," *Neurologic clinics,* pp. 61-84, 1996.

[14] Kwan P, Arzimanoglou A, Berg A T, et al., "Definition of drug resistant epilepsy: consensus proposal by the ad hoc Task Force of the ILAE Commission on Therapeutic Strategies," *Epilepsia,* pp. 1069-1077, 2010.

[15] R. C. Knowlton, "The role of FDG-PET, ictal SPECT, and MEG in the epilepsy surgery evaluation," *Epilepsy & Behavior,* pp. 91-101, 2006.

[16] Knowlton R C, Elgavish R A, Bartolucci A, et al., "Functional imaging: II. Prediction of epilepsy surgery outcome," *Annals of neurology,* pp. 35-41, 2008.

[17] Van Nieuwenhuyse B, Raedt R, Sprengers M, et al., "The systemic kainic acid rat model of temporal lobe epilepsy: Long-term EEG monitoring," *Brain research,* pp. 1-11, 2015.

[18] B. Edward, "The relevance of kindling for human epilepsy[J]. Epilepsia," *Epilepsia,* pp. 65-74, 2007.

[19] M. J. O, "Kindling model of epilepsy," *Advances in neurology,* pp. 303-318, 1986.

[20] Reddy D S, Kuruba R., "Experimental models of status epilepticus and neuronal injury for evaluation of therapeutic interventions," *International journal of molecular sciences,* pp. 18284-18318, 2013.

[21] Curia G, Longo D, Biagini G, et al., "The pilocarpine model of temporal lobe epilepsy," *Journal of neuroscience methods,* pp. 143-157, 2008.

[22] Lévesque M, Avoli M., "The kainic acid model of temporal lobe epilepsy," *Neuroscience & Biobehavioral Reviews,* pp. 2887-2899, 2013.

[23] Ben-Ari Y, Tremblay E, Riche D, et al. , "Electrographic, clinical and pathological alterations following systemic administration of kainic acid, bicuculline or pentetrazole: metabolic mapping using the deoxyglucose method with special reference to the pathology of epilepsy," *Neuroscience,* pp. 1361-1391, 1981.

[24] Amaro Jr E, Barker G J., "Study design in fMRI: basic principles," *Brain and cognition,* pp. 220-232, 2006.

[25] Howseman A M, Bowtel R W., "Functional magnetic resonance imaging: imaging techniques and contrast mechanisms," *Philosophical Transactions of the Royal Society B: Biological Sciences,* pp. 1179-1194, 1999.

[26] Khoo V S, Dearnaley D P, Finnigan D J, et al., "Magnetic resonance imaging (MRI): considerations and applications in radiotherapy treatment planning," *Radiotherapy and Oncology,* pp. 1-15, 1997.

[27] Blink, E. J., "mri: Physics," *Online PDF .*

[28] Matthews P M, Jezzard P. , "Functional magnetic resonance imaging," *Journal of Neurology, Neurosurgery & Psychiatry,* pp. 6-12, 2004.

[29] Kamil Uludag, David J.Dubowitz and Richard B.Buxton, "Basic principles of functional MRI," in *Clinical MRI* , pp. 249-287.

[30] Martin A.Lindquist, and Tor D.Wager, "Principles of functional Magnetic Resonance Imaging," in *Handbook of Neuroimaging Data Analysis*, 2014.

[31] Kang J K, Bénar C G, Al-Asmi A, et al., "Using patient-specific hemodynamic response functions in combined EEG-fMRI studies in epilepsy," *Neuroimage,* pp. 1162-1170, 2003.

[32] M. S. Cohen, " Echo-planar imaging (EPI) and functional MRI," *Functional MRI,* pp. 137-148, 1998.

[33] Petersen S E, Dubis J W. , "The mixed block/event-related design," *Neuroimage,* pp. 1177-1184, 2012.

[34] Ombao, Hernando, et al., Handbook of Neuroimaging Data Analysis, CRC Press, 2016.

[35] D. Mastrovito, "Interactions between resting-state and task-evoked brain activity suggest a different approach to fMRI analysis," *Journal of Neuroscience,* pp. 12912-12914, 2013.

[36] Limotai C, Mirsattari S M., "Role of functional MRI in presurgical evaluation of memory function in temporal lobe epilepsy," *Epilepsy research and treatment,* 2012.

[37] Niethammer M, Feigin A, Eidelberg D., "Functional neuroimaging in Parkinson's disease," *Cold Spring Harbor perspectives in medicine,* 2012.

[38] Rombouts, Serge ARB, Frederik Barkhof, and Philip Scheltens, eds., Clinical applications of functional brain MRI, Oxford University Press, 2007.

[39] D. J. A., "fMRI: applications in epilepsy," *Epilepsia,* pp. 26-31, 2004.

[40] Bashir A, Lipton R B, Ashina S, et al., "Migraine and structural changes in the brain A systematic review and meta-analysis," *Neurology,* pp. 1260-1268, 2013.

[41] Li T Q, Wang Y, Hallin R, et al., "Resting-state fMRI study of acute migraine treatment with kinetic oscillation stimulation in nasal cavity," *NeuroImage: Clinical,* pp. 451-459, 2016.

[42] Kagadis G C, Loudos G, Katsanos K, et al., "In vivo small animal imaging: current status and future prospects," *Medical physics,* pp. 6421-6442, 2010.

[43] Tremoleda J L, Kerton A, Gsell W., "Anaesthesia and physiological monitoring during in vivo imaging of laboratory rodents: considerations on experimental outcomes and animal welfare," *EJNMMI research,* 2012.

[44] Pawela C P, Biswal B B, Hudetz A G, et al., "A protocol for use of medetomidine anesthesia in rats for extended studies using task-induced BOLD contrast and resting-state functional connectivity," *Neuroimage,* pp. 1137-1147, 2009.

[45] Sleigh J, Harvey M, Voss L, et al., "Ketamine–More mechanisms of action than just NMDA blockade," *Trends in anaesthesia and critical care,* pp. 76-81, 2014.

[46] Mitchell R L C, Elliott R, Woodruff P W R., "fMRI and cognitive dysfunction in schizophrenia," *Trends in cognitive sciences,* pp. 71-81, 2001.

[47] L. N. K, "What we can do and what we cannot do with fMRI," *Nature,* p. 869, 2008.

[48] Keilholz S D, Magnuson M E, Pan W J, et al., "Dynamic properties of functional connectivity in the rodent," *Brain connectivity,* pp. 31-40, 2013.

[49] Sakoğlu Ü, Pearlson G D, Kiehl K A, et al., "A method for evaluating dynamic functional network connectivity and task-modulation: application to schizophrenia," *Magnetic Resonance Materials in Physics, Biology and Medicine,* pp. 351-366, 2010.

[50] Kiviniemi V, Vire T, Remes J, et al., "A sliding time-window ICA reveals spatial variability of the default mode network in time," *Brain connectivity,* pp. 339-347, 2011.

[51] Allen E A, Damaraju E, Plis S M, et al., "Tracking whole-brain connectivity dynamics in the resting state," *Cerebral cortex,* pp. 663-676, 2014.

[52] Ray S, Turi R H., "Determination of number of clusters in k-means clustering and application in colour image segmentation," in *Proceedings of the 4th international conference on advances in pattern recognition and digital techniques*, 1999.

[53] Demirtaş M, Tornador C, Falcon C, et al., "Dynamic functional connectivity reveals altered variability in functional connectivity among patients with major depressive disorder," *Human brain mapping,* pp. 2918-2930, 2016.

[54] Contreras J A, Goñi J, Risacher S L, et al., "The structural and functional connectome and prediction of risk for cognitive impairment in older adults," *Current behavioral neuroscience reports,* pp. 234-245, 2015.

[55] Hindriks R, Adhikari M H, Murayama Y, et al., "Can sliding-window correlations reveal dynamic functional connectivity in resting-state fMRI?," *Neuroimage,* pp. 242-256, 2016.

[56] Ashburner J, Barnes G, Chen C, et al., "SPM12 manual," *Wellcome Trust Centre for Neuroimaging, London, UK,* 2014.

[57] Wang J, Wang X, Xia M, et al., "GRETNA: a graph theoretical network analysis toolbox for imaging

connectomics," *Frontiers in human neuroscience,* p. 386, 2015.

[58] Jenkinson M, Smith S M., "Pre-Processing of BOLD FMRI Data".

[59] K. P. Miyapuram, "Introduction to fMRI: experimental design and data analysis," 2008.

[60] Hutchison R M, Womelsdorf T, Allen E A, et al., " Dynamic functional connectivity: promise, issues, and interpretations," *Neuroimage,* pp. 360-378, 2013.

[61] Damaraju E, Allen E A, Belger A, et al., " Dynamic functional connectivity analysis reveals transient states of dysconnectivity in schizophrenia," *NeuroImage,* pp. 298-308, 2014.

[62] Wikipedia contributors., ""Coefficient of variation."," Wikipedia. The Free Encyclopedia, [Online]. Available: https://en.wikipedia.org/w/index.php?.

[63] McKnight P E, Najab J., "Mann-Whitney U Test," *The Corsini encyclopedia of psychology,* pp. 1-1, 2010.

[64] Luo C, Li Q, Lai Y, et al., "Altered functional connectivity in default mode network in absence epilepsy: a resting-state fMRI study," *Human brain mapping,* pp. 438-449, 2011.

[65] Henkin Y, Sadeh M, Kivity S, et al., "Cognitive function in idiopathic generalized epilepsy of childhood," *Developmental medicine and child neurology,* pp. 126-132, 2005.

[66] Bettus G, Guedj E, Joyeux F, et al., "Decreased basal fMRI functional connectivity in epileptogenic networks and contralateral compensatory mechanisms," *Human brain mapping,* pp. 1580-1591, 2009.

[67] Williams K A, Magnuson M, Majeed W, et al., "Comparison of α-chloralose, medetomidine and isoflurane anesthesia for functional connectivity mapping in the rat," *Magnetic resonance imaging,* pp. 995-1003, 2010.

[68] Liu F, Wang Y, Li M, et al., "Dynamic functional network connectivity in idiopathic generalized epilepsy with generalized tonic–clonic seizure," *Human brain mapping,* pp. 957-973, 2017.

[69] Otte W M, Dijkhuizen R M, van Meer M P A, et al. , "Characterization of functional and structural integrity in experimental focal epilepsy: reduced network efficiency coincides with white matter changes," *PLoS One,* 2012.

[70] Leonardi N, Van De Ville D., "On spurious and real fluctuations of dynamic functional connectivity during rest," *Neuroimage,* pp. 430-436, 2015.

[71] Shirer W R, Ryali S, Rykhlevskaia E, et al. , "Decoding subject-driven cognitive states with whole-brain connectivity patterns," *Cerebral cortex,* pp. 158-165, 2012.

[72] Cribben I, Haraldsdottir R, Atlas L Y, et al., "Dynamic connectivity regression: determining state-related changes in brain connectivity," *Neuroimage,* pp. 907-920, 2012.

[73] Bassett D S, Wymbs N F, Porter M A, et al., "Dynamic reconfiguration of human brain networks during learning," *Proceedings of the National Academy of Sciences,* 2011.

[74] Cribben I, Haraldsdottir R, Atlas L Y, et al., "Dynamic connectivity regression: determining state-related changes in brain connectivity," *Neuroimage,* pp. 907-920, 2012.

Annexes

Annexes A

Table A: Top ten connections of ROIs for all states

Rank	1	2	3	4	5	6	7	8	9	10
S1	SSC_l, SSC_r	Sep_l, Sep_r	Cg_l, Cg_r	MC_r, SSC_r	MC_l, SSC_l	MC_l, SSC_r	SSC_l, MC_r	SSC_r, Vis_r	MC_l, MC_r	SSC_r, Hip_r
S2	Sep_l, Sep_r	SSC_l, SSC_r	Cg_l, Cg_r	MC_r, SSC_r	MC_l, SSC_l	MC_l, SSC_r	MC_l, MC_r	SSC_l, MC_r	SSC_l, Th_l	SSC_r, Hip_r
S3	Sep_l, Sep_r	Cg_l, Cg_r	SSC_l, SSC_r	MC_r, SSC_r	MC_l, MC_r	MC_l, SSC_l	SSC_r, Hip_r	MC_l, SSC_r	SSC_r, Vis_r	SSC_l, Hip_r
S4	SSC_l, SSC_r	Cg_l, Cg_r	Sep_l, Sep_r	MC_r, SSC_r	MC_l, MC_r	MC_l, SSC_r	MC_l, SSC_l	CPU_r, SSC_r	SSC_l, CPU_r	SSC_r, Th_r
S5	SSC_l, SSC_r	Cg_l, Cg_r	Sep_l, Sep_r	MC_l, SSC_r	MC_l, SSC_l	MC_r, SSC_r	MC_l, MC_r	SSC_l, MC_r	SSC_r, Hip_r	SSC_r, Th_r
S6	Sep_l, Sep_r	SSC_l, SSC_r	MC_r, SSC_r	Cg_l, Cg_r	MC_l, SSC_r	SSC_l, MC_r	MC_l, SSC_l	CPU_r, SSC_r	MC_r, Cg_r	SSC_r, Vis_r
S7	Sep_l, Sep_r	Au_l, Au_r	SSC_l, Th_l	Cg_l, Cg_r	SSC_l, RSC_l	Hip_l, RSC_l	Th_l, Hip_l	SSC_l, Hip_l	MC_r, Hip_r	GP_l, GP_r

Annexes B

Label Mask

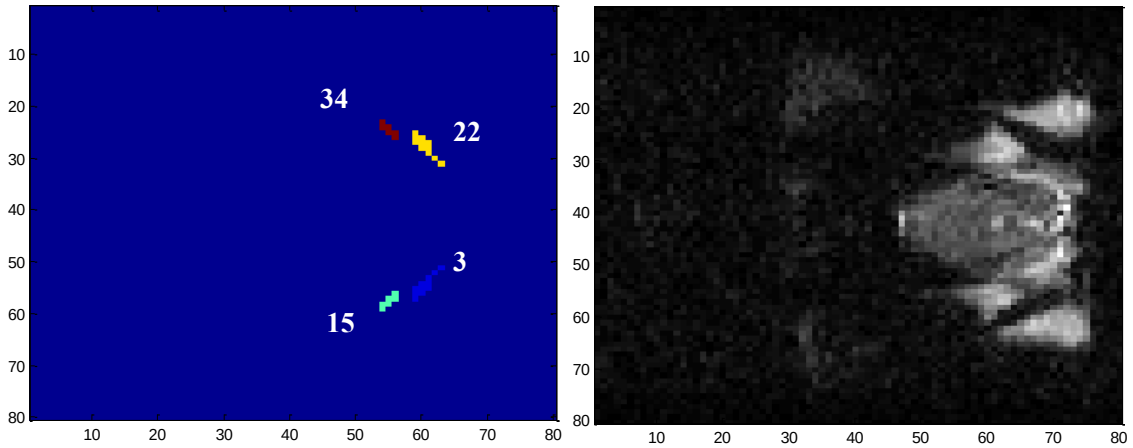

Figure B.1: The 4th slice of label mask (left) and corresponding fMRI image (right)

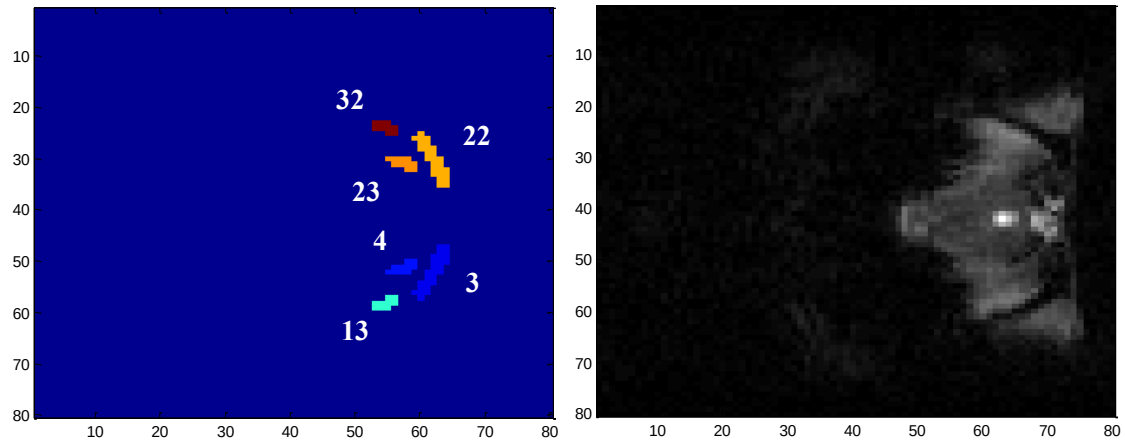

Figure B.2: The 5th slice of label mask (left) and corresponding fMRI image (right)

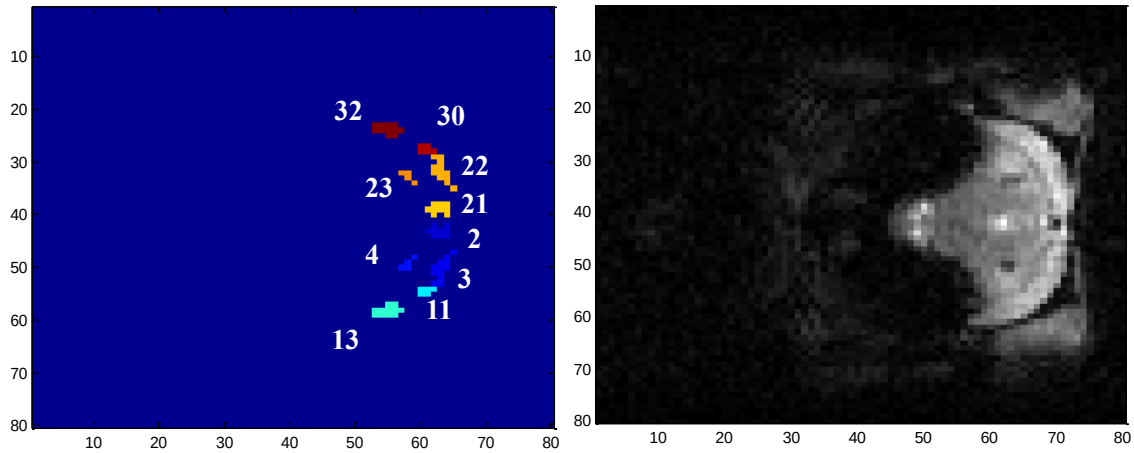

Figure B.3: The 6th slice of label mask (left) and corresponding fMRI image (right)

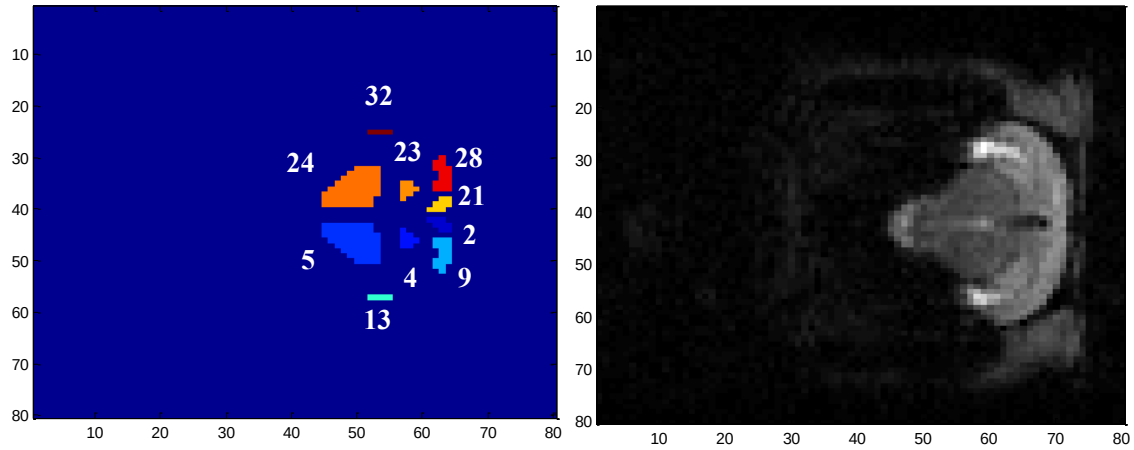

Figure B.4: The 7th slice of label mask (left) and corresponding fMRI image (right)

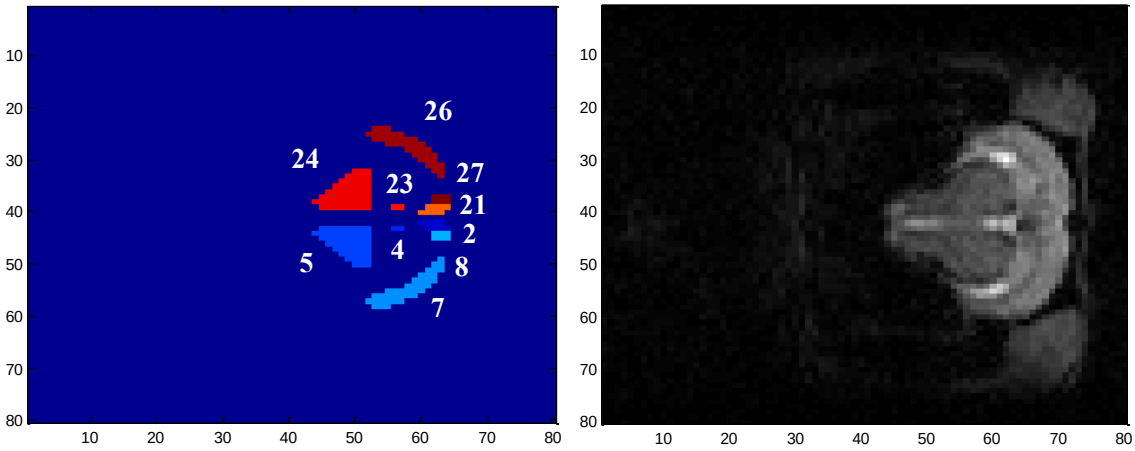

Figure B.5: The 8th slice of label mask (left) and corresponding fMRI image (right)

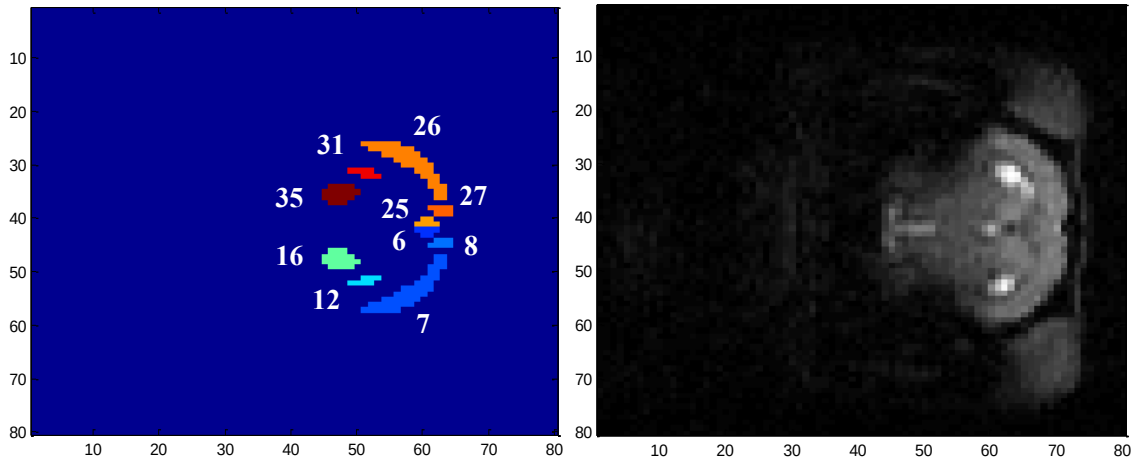

Figure B.6: The 9th slice of label mask (left) and corresponding fMRI image (right)

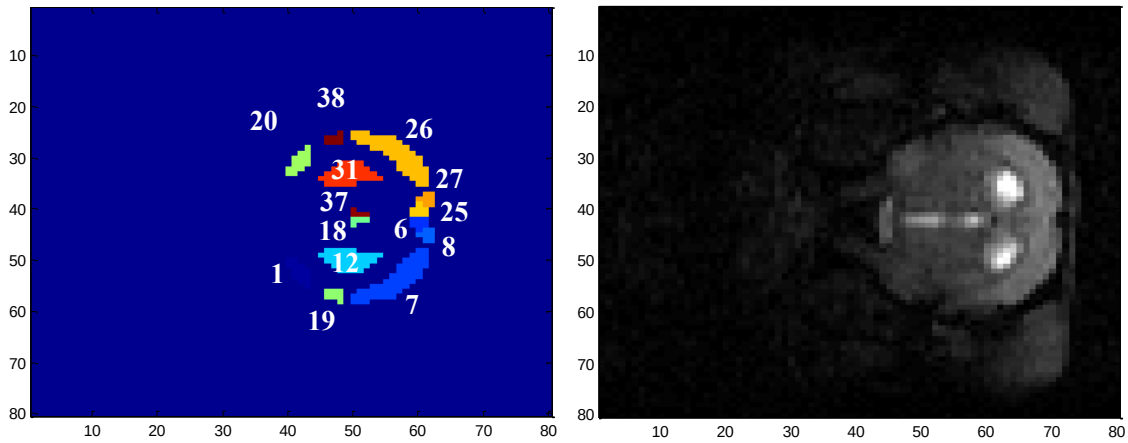

Figure B.7: The 10th slice of label mask (left) and corresponding fMRI image (right)

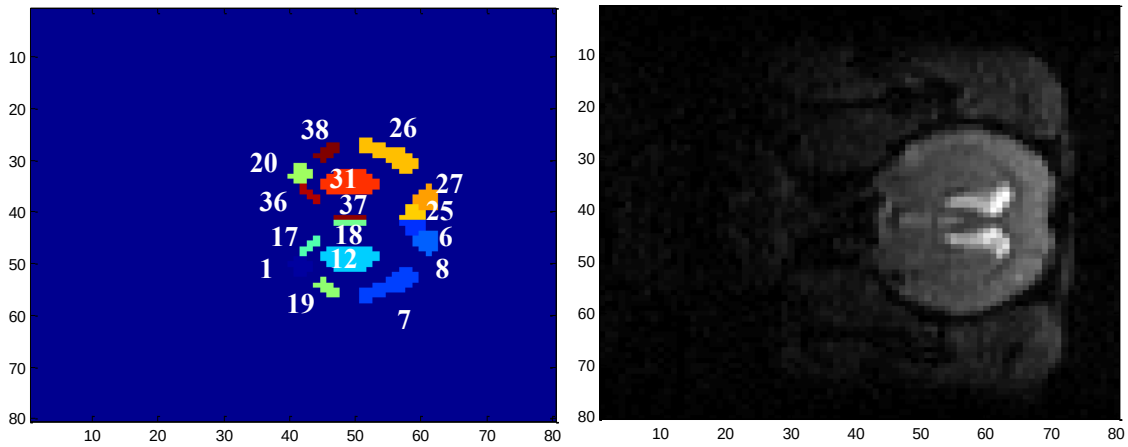

Figure B.8: The 11th slice of label mask (left) and corresponding fMRI image (right)

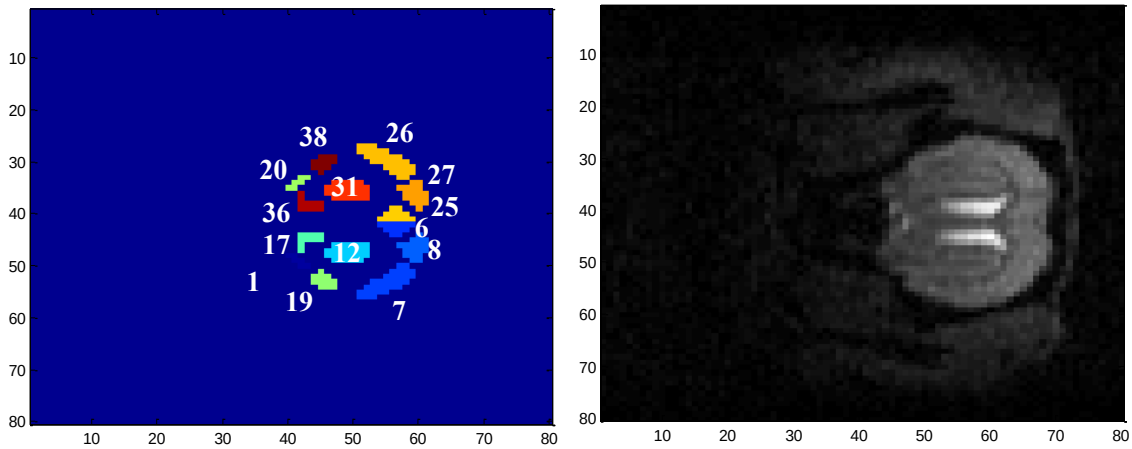

Figure B.9: The 12th slice of label mask (left) and corresponding fMRI image (right)

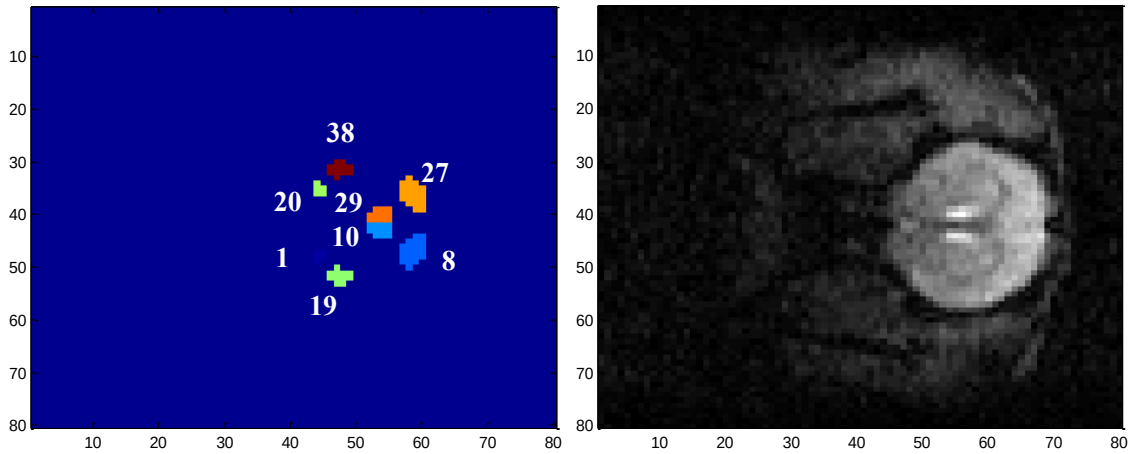

Figure B.10: The 13th slice of label mask (left) and corresponding fMRI image (right)

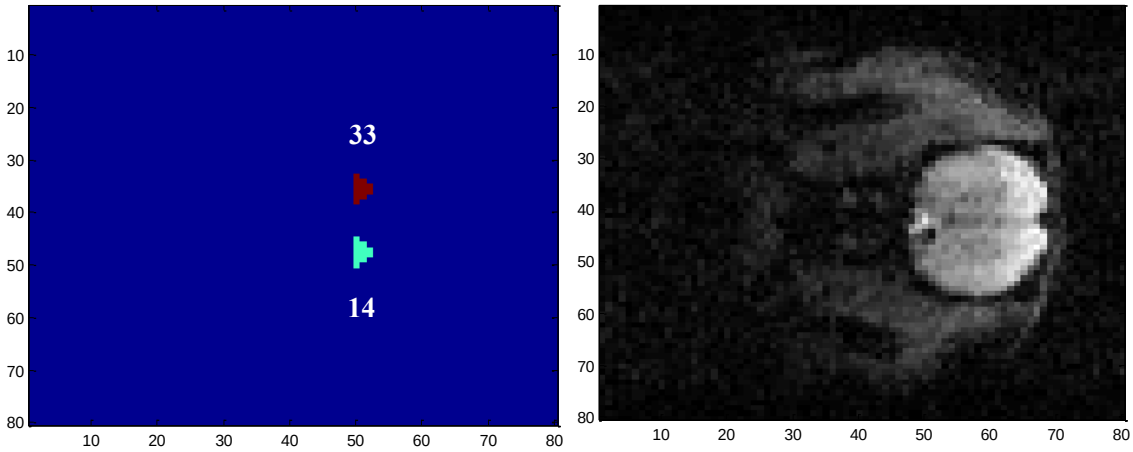

Figure B.11: The 14th slice of label mask (left) and corresponding fMRI image (right)